SPATIAL AND TEMPORAL PATTERNS OF WATER CONTENT IN DRYLAND CROP PRODUCTION IN THE PALOUSE

A Thesis

Presented in Partial Fulfillment of the Requirements for the

Degree of Master of Science

with a

Major in Soil and Land Resources

in the

College of Graduate Studies

University of Idaho

by

Meghan J. Wessel

May 2014

Major Professor: Robert Heinse, Ph.D.

Authorization to Submit Thesis

This thesis of Meghan Wessel, submitted for the degree of Master of Science with a Major in Soil and Land Resources and titled "Spatial and Temporal Patterns of Water Content in Dryland Crop Production in the Palouse," has been reviewed in final form. Permission, as indicated by the signatures and dates below, is now granted to submit final copies to the College of Graduate Studies for approval.

Major Professor:	________________________________	Date:	________
	Robert Heinse, Ph.D.		
Committee Members:	________________________________	Date:	________
	Jodi Johnson-Maynard, Ph.D.		
	________________________________	Date:	________
	David Huggins, Ph.D.		
Department Administrator:	________________________________	Date:	________
	Paul McDaniel, Ph.D.		
Discipline's College Dean:	________________________________	Date:	________
	Larry D. Makus, Ph.D.		

Final Approval and Acceptance

Dean of the College of Graduate Students:	________________________________	Date:	________
	Jie Chen, Ph.D.		

Abstract

Common methods for measuring soil moisture disturb the soil and do not represent large areas with varying topography. We estimated volumetric water content (VWC) using apparent electrical conductivity (EC_a) while comparing chisel plow tillage and no-till as well as crop rotations on a split-plot design. Weekly measurements of EC_a were converted to VWC using multiple linear regression ($r = 0.89$, $p = 0.0$) with the additional variables growing degree days, elevation, clay content, and silt content using a principal component analysis. VWC and EC_a were well correlated ($r = 0.60$, $p = 2.2x10^{-12}$); with a similar percent decrease from April to October. Spring peas retained the highest predicted VWC, followed by spring barley and winter wheat. The spatial and temporal maps of moisture content provided a comprehensive view of the amount, location, and timing of volumetric water content as a function of agronomic management practices.

Acknowledgments

I would like to thank my advisor, Dr. Robert Heinse for his never ending support and positive attitude through this process. His guidance, wisdom, and assistance were of utmost importance to the creation and completion of the research and this thesis and were greatly appreciated. The University of Idaho's Soil and Land Resources Division is full of great professors that I am very grateful to have had the opportunity to learn from.

For soil sample data analysis, I would like to thank Anita Falen for her hard work, Ames Fowler for helping to collect data on long, hot summer days, Mark Corrao for helping in the lab, and for all graduate students that have been along my side in the process.

A special thanks goes to my family and friends' continual encouragement and support from home.

Dedication

I would like to dedicate my thesis to loved ones that have passed: my mother, Alice Wessel, Grandma Betty, Grandma Loos, Aunt Alice and Uncle Mac, and to my grandfathers. They, especially Grandma Betty and the memories of my mother, have played a large role in shaping me into the person I am today. This accomplishment would not have been possible without them.

"Learning is not attained by chance, it must be sought for with ardor and attended to with diligence" – Abigail Adams

Table of Contents

List of Figures

List of Tables

Chapter 1. Introduction

Dryland winter wheat is the staple crop for farmers in the Palouse, an area with a landscape of rolling loess hills within southeastern Washington and north central Idaho. Farmers depend on stored soil water from precipitation in winter and spring months as summers bring higher temperatures and minimal rain. With the lack of summer precipitation, spring moisture accumulation is important to sustain plant growth over the growing season (Singh et al., 2011). Climate change in the inland Pacific Northwest could alter the spatial distribution and timing of soil water patterns and ultimately impact winter wheat yields in the area (Elsner et al., 2010), creating the need to collect temporal soil water distribution data.

The dependence of soil moisture distribution on topography and soil properties is guided by seasonal changes in precipitation and vegetation. Topography based surface and subsurface lateral flow is a main determinant in water flow and distribution in wet spring months (Western, 1998; Zhu, et al., 2010). Soil properties become a larger factor in unsaturated soil water conditions based on soil texture, porosity, and hydraulic conductivity as runoff and saturated flow decreases (Vereecken et al., 2013). In the Palouse, Ibrahim and Huggins (2011) found that elevation and the topographic wetness index (upper slope-dependent water accumulation) were the most influential variables in determining soil moisture distribution in the spring months. They determined that soil properties, such as apparent electrical conductivity and bulk density, were more dominant with the onset of summer and drier conditions. Despite these general trends, correlations between topography, soil properties, and water distribution are site specific (Corwin and Lesch, 2005a, b). Site specific water accumulation in the Palouse is also influenced by snow accumulation and agronomic practices. For example, Qiu, et al. (2011) found that when more residue is left on a crop field with rolling hill topography, snow accumulation tends to be more evenly distributed across the landscape. In contrast, conventional tillage fields, with little residue to hold the snow water in place, showed larger spatial variation for snow accumulation. This likely leads to a larger variation across the landscape of stored soil water (Qiu, et al., 2011). Another topographical feature, aspect, is important for understanding the distribution of water on rolling hill topography. South facing aspects of the rolling hills dry faster in summer months compared to north facing slopes due to the angle of the sun, more direct sunlight, and increased evaporation (Brooks et al., 2012). In addition, vegetative growth can be an indicator of soil moisture fluctuations and including vegetation type and distribution would increase the reliability of topographically based water prediction models (Hupet and Vanclooster, 2002; Wilson, 2005). With changes across the landscape, it is important to analyze the correlation of spatial and temporal water content in regards to soil properties, vegetation, and topographical features.

Vegetation and agronomic practices, such as crop rotations, are impacted by site-specific factors, such as precipitation and aspect, adding complexity to understanding soil moisture distribution on crop fields. With the positive correlation between soil-water storage and wheat yield (Fuentes et al., 2003; Machado et al., 2008), annual variation in precipitation leads to less predictable yields (Schillinger and Papendick, 2008). Understanding variations in soil water content across the landscape will benefit crop yield potential. In the Palouse, there is an east-west gradient with increasing annual precipitation eastward (Brooks, et al., 2012). Locations with higher precipitation, have a rotation of spring wheat or barley and a legume, such as peas, built into their three year rotation (Schillinger and Papendick, 2008) in addition to the main crop, which is winter wheat. Crop rotations are not used in areas where water is limiting as barley and/or peas would deplete soil moisture for the following year. Locations on the western side of the Palouse, with less precipitation, have a year of fallow implemented before wheat planting to maintain higher soil water content and greater wheat yields (Payne et al., 2001; Fuentes et al., 2003). Even in areas with adequate mean-annual precipitation, water conservation remains a concern for the latter portion of the dry season, specifically on ridge tops and south facing slopes (Papendick, 1987). Spring wheat and barley have been shown to deplete soil water to a greater extent than winter wheat (Schillinger and Papendick, 2008; Qi et al., 2013), leaving less water for the successional year. For this reason, spring peas, which are less water intensive (Miller et al., 2006), are planted before a rotational winter wheat year in order to maintain sufficient soil water.

Another agronomic factor, tillage practice, may influence soil water distribution. The increased use of no-till or conservation tillage practices in the Palouse – for the purpose of reduction in soil erosion – could lead to some benefits from added residue. These benefits, such as increased infiltration and reduced evaporation, help maintain higher soil-water storage (Williams, 2011; Su et al. 2007; Fuentes et al., 2003). However, many farmers remain hesitant to move to this type of system for fear of reduced yields (Schillinger and Papendick, 2008). A few studies show that no-till agriculture produces 80%

of the yields of conventional tillage. However, most studies have shown that this is not a consistent correlation and yields under no-till management are no different than those measured under conventional tillage (Cochran et al., 1982; Lafond et al., 1992; Payne et al., 2001; Fuentes, et al., 2003; Machado et al., 2008). Furthermore, studies addressing tillage-based soil moisture differences do not always show no till as having greater soil moisture storage than conventional tillage. In a 2 year study of 2 wheat fields, Riar et al., (2010) found that seed-zone soil moisture (9-11 cm) was greater under conventional tillage for one of the two years for one field, but soil moisture was not significantly different based on tillage practices for the other field/year(s). In addition, there was greater soil moisture in the no till section of one field at depth (60 – 150 cm) for one of the years but the difference was not significant for the other field/year(s). Machado et al. (2008) showed increased soil moisture for wheat in the upper 30 cm for reduced tillage and more soil moisture for all other depths to 150 cm for conventional tillage. For peas, they found that reduced tillage consistently had greater soil moisture at all depths, suggesting trends are crop dependent. The influence of tillage practice on soil moisture content is unclear in wheat fields and may also be site specific.

As discussed, soil water storage fluctuates temporally and spatially (Eagleson, 1978) due to climate (Seneviratne et al., 2010), heterogeneity of soil profiles (Sheets and Hendrickx, 1995), topography (Burt and Butcher, 1985), and vegetation (Eagleson, 1978; Cassiani et al., 2012), resulting in the need for wide-scale water measurements. The majority of studies addressing soil water storage are conducted on a point scale, with data collections at specified locations across a field. These techniques, which use soil sampling (e.g. gravimetric) or some form of soil-water sensing (e.g. time domain reflectometry), are time intensive and intrusive. Hupet and Vanclooster (2002) found that between 2 and 33 samples per 6300 m^2 (1.6 ac) were needed in order to predict mean soil moisture at a given depth with 95% confidence on a relatively flat field. Varying topography adds to the complexity and makes comparisons of point scale data difficult (Tromp-van Meerveld and McDonnell, 2009; Robinson et al., 2012). In the Palouse, this variation in soil moisture would likely require more extensive data collection due to the rolling hill topography. With elevation, landscape position (e.g. shoulder, toeslope), aspect, and slope varying across the hills, it would be difficult for farmers or researchers to maintain this many sample sites for water monitoring.

Spatial scale monitoring of soil moisture is important for precision agriculture (Corwin and Lesch, 2003). Geographic information systems (GIS) are generally paired with other measurement techniques to apply and monitor soil nutrients and properties (Western et al., 2002). Of particular interest for this study is the determination of soil moisture distribution. Due to the difficulties of collecting and interpolating point-scale soil moisture, remote sensing techniques (RST) could provide a more spatial, data intensive alternative (Kornelsen and Coulibaly, 2013). Normalized Difference Vegetation Index (NDVI), which measures vegetative growth, is correlated to soil moisture content (Wang, 2007). Nonetheless, since plant growth is required for NDVI measurements, NDVI would not be able to be used before crop planting to determine soil stored in the profile. RSTs that use microwave wavelengths, such as synthetic aperture radar (SAR), use satellites to determine the dielectric constant, soil surface roughness, and vegetation distribution

(Kornelsen and Coulibaly, 2013). The dielectric constant is highly related to soil moisture content (Kornelsen and Coulibaly, 2013). However, these types of RSTs only gather soil moisture data in the upper few cm (Western et al., 2002), which is not useful for determining soil moisture storage for crops in dryland agriculture.

Electromagnetic induction (EMI) could provide a better means of efficiently measuring spatial and temporal water distribution. EMI is used to determine the apparent electrical conductivity (EC_a) of the soil, such as with the CMD-1 (GF Instruments, Brno, Czech Republic) conductivity meter or, similarly, EM-38 (Geonics, Leighton Buzzard, United Kingdom). These devices are not invasive and can be carried or pulled behind a four wheeler or other similar vehicle as long as they remain consistently close to the soil surface (McNeill, 1980). The effective depth of signal penetration is 0.75 or 1.5 meters for the CMD-1. This is an important depth for being able to quantify soil moisture storage in the root zone (Corwin and Lesch, 2005a). An electromagnetic field given off by the receiver interacts with conductive properties of the soil to induce a secondary magnetic field and is relayed to the receiver with the primary magnetic field. A value of electrical conductivity, termed apparent electrical conductivity (EC_a), is outputted for every measurement point. Measured EC_a is influenced by soil properties that are conductive, such as salinity, soil water content, and clay content (Corwin and Lesch, 2005a, b). The high cation exchange capacity of clay generally means its outer surface is largely negatively charged. Cations such as calcium, magnesium, potassium, or hydrogen ions are attracted to and adsorb to clay's surface, making the clay mineral conductive. Since dissolved solutes remain a necessary part of soil water, soil water content can be correlated to the conductivity readings by the EMI device. In the absence of saline soils, the EC_a has been shown to be linearly related to water content (Rhoades et al., 1976; Sheets and Hendrickx, 1995; Khakural et al., 1998; Tromp-van Meerveld and McDonnell, 2009), but topographic and soil properties, such as clay content should still be used for calibration of EC_a data (Corwin and Lesch, 2003; Corwin and Lesch, 2005b). In California, Sheets and Hendrickx (1995) and in Missouri, Sudduth et al. (2001) found that the spatial EC_a measurements using EMI represent soil water more accurately when done temporally. Temporal maps allow the identification of changes in EC that correlate to water content, while soil properties such as clay content remain constant (Robinson et al., 2009; Robinson et al., 2012). On hilly terrain, topographic measurements are also useful for the prediction of water content (Sauer, et al., 2013). Topographical data can be calculated based on the geo-referenced electrical conductivity data points given by the EMI device.

Objectives

Soil moisture determinations for optimizing crop yield would benefit from more complete spatial and temporal maps of water, climate, and topographic features. The specific objectives of this study were to (1) analyze the tillage and crop system comparisons in terms of spatial and temporal EC_a and EC_a predicted water distribution, and (2) determine site-specific impacts of topographic and soil properties on distribution of EC_a and soil water content and (3) predict temporal and spatial volumetric water content using EC_a and correlated features. For this study the EMI conductivity meter was used to measure EC_a of the soil and determine a relationship to total soil water content. A comparison of tillage system, as no-till versus chisel plow tillage, as well as crop system, with a rotation of winter wheat, spring peas, and spring barley, was made.

Chapter 2. Material and Methods

Field Location, Climate, and Soil Descriptions

The study was conducted at an experimental field on the University of Idaho Kambitsch Farm near Genesee, ID, USA. The farm is in the Palouse region (Fig. 1) of northern Idaho characterized by a mesic temperature regime (Soil Survey Staff, 2010) with a mean annual temperature of 8.5^{o}C with cold winters and hot summers (Western Regional Climate center, 2012). Although the mean effective precipitation is 605 mm/yr (Western Regional Climate Center, 2012), being in a xeric precipitation regime (Soil Survey Staff, 2010), the majority of the precipitation occurs during winter and spring months (Fig. 2). During our study, the annual precipitation was 591 mm in 2012 (Western Regional Climate Center, 2013). The dominating soil series is a Palouse silt loam classified by the NRCS as a Fine-silty, mixed, superactive, mesic Pachic Ultic Haploxeroll (Soil Survey Staff, 2010). The fine textures, high cation exchange capacity, and deep A horizon of a Mollisol give the soil naturally high fertility and high water holding capacity. The depth to water table is generally over 200 cm deep (Soil Survey Staff, 2010).

Experimental Design

The 3.9 acre experimental field (192 x 82 m) is managed as a split plot design with alternating rows perpendicular to the slope testing both tillage management and crop rotations as shown in Fig. 3. Tillage treatments were chisel plow (CP) and no-till (NT). The CP and NT main plots alternated going up the hillslope, starting with NT at the foot slope and ending with CP on the shoulder of the top of the field, for a total of ten plots. Within each CP or NT plot there was one subplot of winter wheat (WW), spring barley (SB), and spring pea (SP) each, giving three subplots within each CP or NT main plot. Each subplot measured 6 m by 82 m with 1.2 m of unplanted soil between each main plot.

Winter wheat (WW) (*Triticum Asetivum*, 528/523 blend) was planted on October 27th, 2011 at a rate of 110 lbs/ac with 260 lbs of 31-10-0-7.5 deep banded dry fertilizer. The entire field was top dressed via a plane with 40-0-0-6 (with chloride) fertilizer on April 9th, 2012 at a rate of 100 lbs per acre. Spring peas (SP) (*Pisum sativum*, Aragorn peas) were planted the following spring on May 14th, 2012 at 120 lbs/ac. Spring barley (SB) (*Hordeum vulgare*) was planted on May 16th, 2012 at 80 lbs/acre with 260 lbs of 31-10-0-7.5 deep banded dry fertilizer applied at the same time. At the end of the growing season, SB averaged 1.94 tons/acre and SP averaged 0.24 tons/ac. The yields in the NT and CP plots were not significantly different. Winter wheat averaged 82.2 bu/ac. CP plots were significantly greater ($p < 0.05$) with yields of 85.7 bu/ac compared to the NT plot yields of 72.6 bu/ac (Bull, 2012).

Spatial measurements of soil variability

We used the non-invasive CMD-1 electromagnetic induction (EMI) conductivity meter (GF Instruments, Brno, Czech Republic) to collect subsurface apparent conductivity (EC_a). The instrument collected a geo-referenced datum (including elevation) every second (approx. every 1.3 m) using a sub-meter accuracy GPS receiver (SX BlueII, Geneq, Montreal, Canada). The EMI instrument was carried at a walking pace between crop rows, perpendicular to the slope, with ~84 cm linear distance between each measurement path.

There were four measurement paths per each subplot. The instrument was held approximately 8 cm above the ground on the vertical co-planar (VCP) setting for an effective depth of approximately 1.5 m (McNeill, 1980). This depth range was chosen to maximize sensitivity to root zone moisture as suggested by Corwin and Lesch (2005). Throughout the 2012 growing season, May to October, thirteen time-lapse field-scale EMI measurements were collected (Fig. 2). Approximately 8,000 apparent electrical conductivity (EC_a) data points were collected per field measurement. The sensed EC_a is a function of depth weighted subsurface electrical conductivity given by the 1-dimensional vertical sensitivity distribution found in McNeill (1980):

$$EC_a = \int_z^{\infty} \phi_V(z)dz \qquad (1)$$

Where z is the depth, V indicates VCP setting, and ϕ is the real conductivity at depth z.

EC_a data were normalized to a reference temperature of 25^{o}C using the equation found in Reedy (2003):

$$EC_{25} = EC_a\left(0.4779 + 1.3801e^{\left(\frac{-T}{25.654}\right)}\right) \qquad (2)$$

In lieu of measured soil temperatures profiles, we estimated the depth-weighted temperature *T* based on the model found in Van Wijk and De Vries (1963) with average air temperature and diurnal amplitude as input parameters derived from daily measurements at the field location weather station. The characteristic damping depth and phase constant were estimated by fitting the model to observations of daily average soil temperatures over one year measured at the 10-cm depth using a standard Levenberg-Marquardt least squares algorithm implemented in Matlab 13b (The Mathworks, Natick, MA, United States). Depth weighing of T used the sensitivity distribution in Eq. (1) to calculate an effective temperature for conversion to EC_{25}. From this point forward EC_a will represent EC_{25} as temperature-corrected apparent electrical conductivity.

A digital elevation model (DEM) was derived by fitting a local linear regression surface to pooled elevation data collected along with the EMI measurements. Slope and aspect were derived from the DEM using scripts in TopoToolbox (Schwanghart and Kuhn, 2010). The topographic wetness index (TWI) was calculated using Beven and Kirkby (1979).

Calibration Data

Soil samples were collected and analyzed to determine volumetric water content (VWC), particle size, soil pH, bulk density, bulk EC and electrical conductivity of the pore fluid (EC_e). Fig. 3 gives the locations of the sixty sampling sites for bulk density and twelve sites used for all other soil samples. Two soil samples per subplot were collected for bulk density determination using a Giddings probe (Giddings Machine Co., Colorado, USA). The samples went to a depth of 100 - 150 cm depending on refusal and were collected on October 31st, 2012. Bulk density was determined in 10 cm increments from 0 to 30 cm and in 30 cm increments from 30 cm to maximum depth. The twelve sampling locations were selected using ESAP-RSSD software (US Salinity Laboratory, California, USA) to optimize sampling design based on a response surface sampling design (Lesch et al., 2000). The response surface sampling design used the spatial variability in EC_a derived from the EMI measurements in the wet state (December 8, 2011) to create a regression model and sample sites that represent the electrical conductivity data (Lesch et al., 2000). At each site, soil samples were collected at 0-10, 10-20, 30-40, 50-60, and 90-100 cm depths with a 2.5 cm diameter soil probe.

Soil texture was determined by pipette procedure using collected soil samples from each of the twelve sites and thirty of the sixty locations (approx. every other location going up the hill) from the bulk density measurements, for a total of 42 samples. Texture analysis was done on the lower and upper 50 cm to a depth of 100 cm. For better accuracy of texture analysis, samples were tested and were negative for carbonates, and had organic matter (Mikhail and Briner, 1978) and excess ions (95% methanol and 95% ethanol washings) removed. Texture analysis was done via pipette procedure per Kilmer and Alexander (1949) based on USDA-NRCS standards for classification.

VWC and bulk EC were measured using a Trime-Pico IPH/T3 soil moisture sensor (IMKO, Etlingen, Germany) starting June 17th, 2012 (Fig. 2). At each of the twelve sites TECANAT PC plastic access tubes were augered without pre-boring to a soil depth of 80 cm. The tubes allowed repeated measurements on days of EMI data collection in 15-cm depth increments.

Soil pH and the electrical conductivity of the pore fluid (EC_e) were determined using the saturated paste extract method (Burt, 2004). EC_e and pH data from soil samples collected on May 8th and May 24th were compared via a paired t-test for differences. The two dates were used as there were fertilizer applications between them and to determine if the fertilizer application impacted the EC_e and pH.

Statistical Analysis

The average EC_a within plots planted to winter wheat (WW), spring barley (SB), and spring peas (SP) under chisel plow (CP) or no-till (NT) management were compared. There were 30 subplots in the field or 10 per crop type and 15 per tillage type, making up 10 total plots with each containing one type of tillage and three crops (Fig. 3). The subplots within a plot were paired together relative to their location on the field and compared with a paired t-test based on average EC_a. This procedure was done for comparing WW to SB, WW to SP, SP to SB, NT to T, and also crop and tillage combinations, such as WW NT to WW T.

Sensor water, VWC, bulk density, and texture were depth weighted based on the sensitivity distribution given by Equation 1. The data was normal-score transformed and fitted with a variogram (Table 1). Univariate ordinary kriging in Spacestat (Biomedware, Michigan, USA, ver. 3.8.5) was used to estimate spatial distributions of elevation, bulk density, clay, silt, and sand percentages as well as EC_a (Table 1). Continuous maps of the variables were created with a back transformation of the kriged data.

We used principal component analysis (PCA) to determine variability in site-specific data using Biomedware's Spacestat. PCA was used to create eigenvectors, or for our purpose condensed variables (CV) of the original measured variables (MVs) and accounts for the original covariance and multicollinearity. A correlation matrix was used to determine the correlation coefficients between the MVs: growing degree days (GDD), elevation, sand, silt, and clay percent, VWC, bulk density, topographic wetness index, slope, and aspect. Since VWC data was collected at the 12 collection sites, data inputted into the PCA was only from these 12 locations for all collection dates (Fig. 3). GDD represents the cumulative GDD starting on April 1st, 2012 and was determined based on the maximum and minimum temperatures taken from the weather station near the field, using $0^{o}C$ as a reference. On dates where temperature data was missing (3% of dates), average temperature from the days before and after were used for calculation. The variables that were highly correlated to VWC and EC_a were used as inputs for PCA.

The resulting CVs and the categorical values, crop and tillage type, were then used in a multiple linear regression to predict VWC for the 12 sites from April to October and compared to the measured VWC. VWC was then predicted for the entire field for all collection dates using the regression equation created with growing degree days (GDD), and kriged elevation, silt, clay, and EC_a.

Chapter 3. Results

Soil properties

Predicted clay, silt, and bulk density distributions are shown in Fig. 4 a-c. Seventy four percent of the field was classified as silty clay loam and 26% was silt loam. The clay percentage ranged from 23 to 37%, with an average of 30%. The lower half of the field had a relatively higher clay content compared to the upper portion of the field, with notably higher clay content on the southeast side. Silt content was greatest on the upper northern half of the field and decreased on the lower half. Silt ranged from 57 to 71% and averaged 64% for all soil samples. Bulk density (BD) was lowest on the upper half of the field and on the lower southwest side and ranged from 1.44 to 1.7 g/cm^3, with an average of 1.61 g/cm^3 (Fig. 4c). BD increased towards the East and midsection of the field, as did clay content. The upper portion of the field had the greatest silt content and lowest clay and BD. The reverse was true for the lower half of the field, except for BD, which varied across the toeslope.

Soil samples collected on May 8th and 24th of 2012 were analyzed to determine the impact of fertilizer application on pH and EC_e. The soil pH and EC_e before and after fertilizer application did not differ significantly for the surface nor any other depth (paired t-test, α=0.05). The average pH for all depths (maximum depth 55 cm) before and after fertilizer application was 4.98 and 4.84, respectively. Specifically, the mean surface pH (0-5 cm) for before and after fertilizer application was 4.51 and 4.53, respectively. The average EC_e for all depths (maximum depth of 55 cm) before and after fertilizer application was

0.34 and 0.40 mS/m, respectively. At the surface, the mean EC_e was 0.40 and 0.35 mS/m, respectively. Due to the relative stability in soil pH and EC_e over time with fertilizer application, they were not included as factors that influence transient EC_a for this field in the PCA and linear regression discussed later.

Agronomic Differences

Kriged maps of EC_a were used to compare agronomic practices (Figs. 5a-g and 6). Patterns of EC_a among crops changed distinctly between the beginning and the end of the growing season (Fig. 6a). Spring rains resulted in slight increases in EC_a between April and June (Figs. 2 and 6a). With precipitation for the growing season ending in July, EC_a began to decrease. From August through October, the EC_a remained at a constant and relatively low value, with no precipitation during these dates (Figs. 2 and 6a). These trends were consistent for all crops (Fig. 6a). At the beginning of the crop season (May – July 2), spring pea (SP) (42 mS m^{-1}) and spring barley (SB) (40 mS m^{-1}) had greater average EC_a compared to winter wheat (WW) (35 mS m^{-1}). At the end of the season (Aug – Oct), SB (23 mS m^{-1}) and WW (23 mS m^{-1}) had lower average EC_a values compared to that measured in SP (28 mS m^{-1}). Between April 17th and June 17th, 2012 SP did not have significantly different EC_a compared to SB (paired t-test, α=0.05). WW EC_a was about 17% less than SP and 12% less than SB from May 24th to July 19th and remained about 19% less than SP EC_a for the majority of the rest of the season. SB EC_a became significantly less than SP EC_a starting on July 11th and continued to be about 18% less for most of the season. In the latter portion of the growing season, from July 30th to October 4th, 2012 WW and SB were not significantly different. On July 30th the EC_a was not significantly different between the different crop sections. Between May 24th and October 4th, 2012, EC_a in WW, SB, and SP subplots decreased by 46%, 43%, and 36%, respectively.

Chisel plow (CP) plots had between 6 and 12% less EC_a than no-till (NT) plots for all collection dates (Fig. 6b). From April to October, average EC_a decreased by 12.3 mS m^{-1} for CP and 12.9 mS m^{-1} for NT. From May 24th to July 30th, average EC_a decreased by 45% in NT plots and 48% in CP plots. From August 19th to October 4th, 2012 neither the CP or NT plots significantly changed (Fig. 6b). The difference in means between EC_a in NT and CP plots ranged from 2.21 and 4.43 mS m^{-1}, with NT maintaining greater EC_a, with the beginning of the season having the largest difference.

Tillage had a stronger influence on EC_a within SB and WW sections as compared to within SP sections (Fig. 7). Between April and July SB NT maintained similar EC_a to SP subplots. SB CP had lower EC_a values than did SB NT and was at about the same level of EC_a as WW NT from May to July. WW CP had the lowest EC_a from May to July. From August to October, SP NT and CP plots maintained the greatest EC_a, followed by SB NT and WW NT, with SB CP and WW CP having similar relatively lower mean EC_a. SB NT had significantly greater average EC_a on April 17th and July 11th, with all other dates having no significant difference between NT and CP SB subplots. Barley NT averaged 32.9 mS m^{-1} while SB CP averaged 28.6 mS m^{-1} from April to October. WW NT had greater average EC_a compared to WW CP subplots on June 10th, July 2nd, July 11th, July 19th, July 30th, August 19th, and September 15th, 2012, with an average of 27.2 mS m^{-1} for CP and 30.4 mS m^{-1} for

NT. SP NT and CP did not have different average EC_a between subplots for any collection date, with an average of 34.2 mS m^{-1} and 33.1 mS m^{-1} across dates, respectively.

Water Prediction

The measured variables (MVs) of GDD, elevation, aspect, slope, TWI, EC_a, VWC, BD, and sand, silt, and clay percent, were compared in a correlation matrix (Table 2). Since the focus of this study was to use EC_a to predict VWC, we focused on the variables correlated to these two variables. EC_a was highly correlated with many of the other variables, contrasting with VWC, which was only highly correlated to 3 of the MVs according to the correlation matrix. The main variables that correlated with EC_a were silt ($r = -0.68$, $p = 1.43 \times 10^{-16}$), clay (-0.65, 6.2×10^{-15}), elevation (-0.63, 1.1×10^{-13}), VWC (0.60, 2.2×10^{-12}), GDD (-0.48, 9.9×10^{-8}), BD (0.40, 1.4×10^{-5}), and TWI (0.30, 1.5×10^{-3}). The main MVs that correlated with VWC were EC_a ($r = 0.60$, $p = 2.2 \times 10^{-12}$), GDD (-0.59, 4.7×10^{-12}), and elevation (-0.34, 2.7×10^{-4}). Slope and aspect were not highly correlated with either EC_a or VWC (slope: $r = 0.19$, $p = 0.02$; $r = -0.06$, $p = 0.56$; aspect $r = 0.19$, $p = 0.05$; $r = -0.12$, $p = 0.20$, respectively).

For the prediction of VWC using a Principal Component Analysis (PCA) the MVs EC_a, GDD, elevation, silt, and clay content were used due to their correlation with VWC and EC_a. In addition, the PCA was done repeatedly with all variables and compared with respect to the correlation coefficient when certain variables were excluded. For example, silt and clay were part of the final PCA as their inclusion resulted in a greater correlation coefficient and therefore prediction of VWC. EC_a, GDD, elevation, silt, and clay content MVs were used in a PCA by creating the 3 CVs that account for 96% of the variability in the data (Table 3).

The CVs were new variables created using the combination of MVs, with the MVs becoming independent of each other. The first CV, which accounted for the most variability in the data (65%) was highly based on several of the variables including, elevation, silt, clay, and EC_a. The second CV was highly influenced by GDD and accounted for an additional 24% of the variability in data. The main contributor to the third CV was elevation and, to a lesser extent, clay content and accounted for another 6.5% of the variability, giving a total of 96% of the variability accounted for in the PCA.

In order to predict spatiotemporal changes in VWC, we used a multiple linear regression using PCA transformations of MVs to condensed variables (CVs) (eigenvectors). The created CVs in combination with crop type were used to create a linear regression equation to predict VWC. Including tillage type in this regression did not increase the predictability of VWC, as evident by no change in the correlation coefficient with its addition, and was not considered significant in the regression ($p > 0.05$) and was therefore not included. A prediction model for VWC in a field with WW, SB, and/or SP gives the following regression equation ($r = 0.89$, $p = 0.0$) (Fig. 9):

$$\theta_v = 24.90497 - 2.25225CV1 - 2.90325CV2 + 2.228952CV3 + 6.304125BV + 9.951404PV$$

where CVs represent the variables created by PCA using a combination of EC_a, GDD, elevation, silt, and clay contents. BV represents whether or not the field was planted with SB (1 for Barley, 0 for no), and PV represents whether or not the field had SP (1 for peas, 0 for no). A 0 for both SB and SP indicates WW.

Predicted VWC from the regression equation was linearly correlated with measured VWC (Fig. 7) and was used to create spatial maps of VWC (Fig. 5 h-n). Predicted VWC distribution maps show many of the same visual horizontal lines as EC_a, generally representing crop type (Figs. 3 and 5). The lines are more abrupt due to the addition of a crop-specific input into the linear regression equation. The overall distribution trends seen in the EC_a maps are seen in the VWC maps. For example, on April 17th, there is an increase in EC_a towards the bottom of the field. Specifically, there are two oblong shaped locations on the lower mid-section of the field with greater conductivity. With a closer look at the predicted VWC map for April 17th, higher water content is seen in these locations as well. The predicted VWC of WW, seen as horizontal lines with lower predicted water, on the lower half of the field make it harder to see this trend. Nonetheless, this area of increased water is maintained over the growing season, as it is in the EC_a maps. While the crop-specific predictions make the horizontal lines more abrupt, they do correspond to the more gradual lines seen in the EC_a distribution maps. There was an abrupt decrease in EC_a and VWC distribution beginning in July. From August to October, a drier state is predicted to be maintained, but it does not stay as constant as the EC_a distribution did and continues to decrease with time due to GDD in the regression equation (Figs. 2, 8, and 9). The average predicted VWC for April 17th was 36.2%. August 19th was predicted to have 27% VWC, a 26% decrease from April 17th. By October 4th, the predicted VWC was down to 24%, a 33% decrease from April 17th. The average EC_a decreased 34% between April 17th and August 19th, 2012 with an average EC_a of 37.1 mS m^{-1} and 24.5 mS m^{-1}, respectively. On the last EC_a collection date, October 4th, 2012, the average EC_a was also 24.5 mS m^{-1}.

Predicted VWC showed distinct differences between crop plots. While a trend can be seen with the NT having greater VWC than CP subplots of SB and WW, the differences were not considered significant (paired t-test, α=0.05). The SP NT and CP subplots maintained 10 and 5% higher VWC than WW and SB, respectively, through the course of the entire season. NT and CP SB also maintain about 5% more VWC compared to the WW NT and CP.

Chapter 4. Discussion

Correlation of variables

For this study, EC_a was shown to be an important factor in the prediction of VWC ($r = 0.60$, $p = 2.2 \times 10^{-12}$) and having a larger impact than GDD, elevation, silt, clay, aspect, TWI, bulk density, or slope ($r = -0.60, -0.34, -0.2, 0.18, -0.12, 0.12, 0.07, -0.06$, respectively). Elevation was the main topographic feature that correlated with EC_a ($r = -0.63$, $p = 1.0 \times 10^{-13}$) and to a lesser extent VWC ($r = -0.34$, $p = 2.7 \times 10^{-4}$). Ibrahim and Huggins (2011) found that topography was the main contributor and EC_a the second most important variable in the prediction of soil water content on a site 25 miles northwest of the Kambitsch farm with similar soil types. The Ibrahim and Huggins study consisted of two EC_a data surveys, before barley planting and after barley harvest. The addition of multiple surveys for this study may increase the correlation between EC_a and VWC prediction as it would better capture changes in EC_a and water content over time. The low correlation between TWI and water and EC_a found by this study was also found by Robinson, et al. (2012). The combination of catchment area and slope was not enough to predict locations of water accumulation. They concluded that TWI would likely be more useful with the incorporation of spatial soil texture. This proved to be successful, as with our study, soil texture was the main correlated factor with EC_a (clay: $r = 0.65$, $p = 6.2 \times 10^{-15}$; silt: $r = -0.68$, $p = 1.4 \times 10^{-16}$), contrasting to VWC which was not well correlated to soil texture (clay: $r = 0.18$, $p = 0.06$; silt: $r = -0.20$, $p = 0.04$). Sand content was not correlated with EC_a or VWC ($r = -0.15$, $p = 0.11$; $r = 0.01$, $p = 0.95$, respectively). Despite the lower correlation with VWC for the entire growing season, soil texture was still an important variable in predicting water. Future use of EC_a for prediction of water should continue to determine the correlation between different factors and soil water content. Each site offers its own unique combination of topographic features and soil properties.

Differences between crops and tillage

Few studies have addressed using EC_a as a comparison for crop rotations and the impact on the soil moisture despite the increased use of EC_a as a non-invasive option for prediction of water content. The large amount of data collected per each subplot (approx. 283 per subplot per date) allowed for greater representation of that subplot when conducting data analysis. Our data showed that this is especially important when analyzing data on a hillslope. For this study the variation in soil properties, VWC, EC_a, and topography features between east and west as well as north and south was apparent. Had there been point scale data, these differences would not have been represented as well.

The EC_a crop comparison results showed SB to be closer to the higher EC_a of SP from April to the beginning of July, when there were still occasional rain events. On July 30th, the SP EC_a did not match its EC_a pattern of the rest of the season. This is likely due to the growth stage of the peas and the difficulty of transporting the EC_a through the tightly wound tendrils causing the EMI meter to be held at a greater distance from the ground. Towards the end of the season, from August to October, during which the soil was drying out, SB was closer in EC_a to WW, which consistently had lower EC_a compared to SP. Whether it remained a significant difference or not, SP maintained the highest EC_a and WW the lowest throughout the growing season. This overall trend was mirrored by the VWC predictions, with SP retaining the highest amount of water, followed by SB, and WW with maintaining the lowest amount of water throughout the growing season.

Since crop type was a factor in the multiple linear regression, the differences in predicted VWC between crops remained constant over the growing season. The variability in EC_a was much greater compared to the VWC predictions. Following a linear regression, the predicted VWC of individual crops slowly decreased with time rather than matching the EC_a temporal changes of more drastic decreases from June to July and remained static from August to October (Compare Figs. 8 and 9). The percent change from April to October was not different between EC_a and predicted VWC for WW, SB, and SP (41, 36, 25% and 41, 33, 28%, respectively; paired t-test, $\alpha = 0.05$). Despite the non-linear EC_a temporal changes contrasting with the linearly predicted VWC, EC_a could be a useful tool for predicting water trends for different crops over time as overall changes between the beginning and end of the season were consistent between the two.

NT and CP sections showed similar trends for the crop subplots in regards to EC_a and VWC prediction maps. NT had greater EC_a and predicted VWC than CP for the entire season, but the difference was only significant for EC_a ($p < 0.05$). The multiple linear regression equation did not have tillage as a specified factor in the analysis, as it did not increase the correlation between measured and predicted VWC. It is possible that PCA and regression analysis did not include tillage practices because the differences in EC_a between crop types was so much greater than the differences for EC_a between tillage practices, suggesting that vegetation has a much larger impact on stored soil water than tillage practices. It could also suggest NT and CP sections have similar rates of change in VWC over the growing season since they follow the same regression equation. The differences between mean EC_a of NT and CP plots increased notably during precipitation events (Fig. 2) (April to July) and decreased during the later portion of the summer (July to October). The changes in differences between CP and NT was minimal and not apparent when looking at the VWC prediction (Fig. 9). It is likely that over time minimal amounts of increased infiltration would cause larger differences between NT and CP (Williams, 2011). Robertson (2010) compared NT and CP soil water content on the same field as this study and showed that it can take 9 years for NT to have greater water content compared to CP. The plot design for Kambitsch farm was changed after the Robertson study was completed and became the current split plot design one year prior to this study. It is suggested that the timeframe of NT conversion be taken into consideration when applying multiple linear regression for prediction of soil water content using EC_a. Farms that have been converted from CP or conventional tillage to NT may require different multiple linear regression equations with time in order to correct for any increased infiltration with NT crop land.

Chapter 5. Summary and Conclusions

This study described how spatial and temporal EC_a data can be used in combination with properties such as elevation, soil texture, crop type, and possibly tillage practices to predict water content over time in dryland agriculture. For our study location, texture (silt and clay content), elevation, and volumetric water content were more correlated than aspect, topographic wetness index, slope, or bulk density was to apparent electrical conductivity, given by the EMI meter. As clay and volumetric water content increased, so did apparent electrical conductivity. In locations of lower silt content and elevation, apparent electrical conductivity measurements were greater. Apparent electrical conductivity, growing degree days, elevation, and texture (silt and clay content) were the most important site-specific variables for prediction of soil water content. Soil water content increased in areas with lower elevation and greater apparent electrical conductivity, and to a lesser extent greater silt content and lower clay content.

The addition of crop type in a model is key to predicting soil water content. We found that spring pea had the greatest retention of soil water at the end of the growing season, followed by spring barley and winter wheat. The differences in soil water content between chisel plow and no-till sections were not as apparent. Pea sections did not show a difference in water between tillage practices. In addition, while winter wheat and spring barley sections consistently had greater soil water content, the differences were not significant. The differences in water content between crop sections was ten times greater than the differences between no-till and chisel plow, causing the difference in crop type to be dominant in the prediction of water. The field had only been in its current crop rotation and tillage set-up for 1 year prior to this study. Other studies with longer term no-till practices would be beneficial to further understand the dynamics between tillage practices and crop rotations on soil water distribution.

The apparent electrical conductivity of crop subsections was more dynamic compared to water content. Spring pea and spring barley subsections had similar apparent electrical conductivity until July. After which, spring pea subsections maintained greater conductivity values for most of rest of the season. Winter wheat subsections, starting with lower conductivity values, maintained the same conductivity as spring barley from July to October. With apparent electrical conductivity changing between crop subsections over the course of the growing season, conductivity based water models would benefit from looking at temporal conductivity changes. The water content and apparent electrical conductivity of the subsections had the same percent decrease between April and October, indicating the potential for apparent electrical conductivity to be able to predict water content changes for the growing season. Future work should include the comparisons between apparent electrical conductivity and soil water content on an annual basis, to better evaluate their differences over time.

Soil water content was able to be effectively predicted based on apparent electrical conductivity and site-specific variables. Using electromagnetic induction-derived apparent electrical conductivity for soil water content prediction will be very useful for farmers that are interested in understanding how their specific location is being impacted by climate change as far as water distribution, depending on their crop type or rotation. Specifically, they could have a better understanding of the timing (length and duration) of spring soil moisture storage and when the soil moisture becomes depleted. Volumetric water content prediction based on apparent electrical conductivity values could also be useful for researchers in the Palouse trying to understand the dynamics of climate change on water distribution spatially and temporally and how different agricultural practices are impacted by any changes.

References

Beven, K.J., and M.J. Kirkby. 1979. A physically based, variable contributing area model of basin hydrology. Hydrological Sciences Bulletin 24(1): 43–69.

Brooks, E.S., J. Boll, and P.A. McDaniel. 2012. Hydropedology in Seasonally Dry Landscapes: The Palouse Region of the Pacific Northwest USA. Hydropedology: Synergistic Integration of Soil Science and Hydrology: 329–350.

Bull, B. 2012. 2012 Tillage Strip Data. Personal Communication via Email.

Burt, R. 2004. Soil survey laboratory methods manual: soil survey investigations report No. 42 Version 4.0. Nebraska: United States Department of Agriculture. Natural Resources Conservation Service.

Burt, T.P., and D.P. Butcher. 1985. Topographic controls of soil moisture distributions. Journal of Soil Science 36(3): 469–486.

Cassiani, G., N. Ursino, R. Deiana, G. Vignoli, J. Boaga, M. Rossi, M.T. Perri, M. Blaschek, R. Duttmann, and S. Meyer. 2012. Noninvasive monitoring of soil static characteristics and dynamic states: a case study highlighting vegetation effects on agricultural land. Vadose Zone Journal 11(3).

Cochran, V.L., L.F. Elliott, and R.I. Papendick. 1982. Effect of Crop Residue Management and Tillage on Water Use Efficiency and Yield of Winter Wheat. Agronomy Journal 74(6): 929–932.

Corwin, D.L., and S.M. Lesch. 2003. Application of Soil Electrical Conductivity to Precision Agriculture. Agronomy Journal 95(3): 455–471.

Corwin, D.L., and S.M. Lesch. 2005a. Apparent soil electrical conductivity measurements in agriculture. Computers and Electronics in Agriculture 46(1–3): 11–43.

Corwin, D.L., and S.M. Lesch. 2005b. Characterizing soil spatial variability with apparent soil electrical conductivity: I. Survey protocols. Computers and Electronics in Agriculture 46(1–3): 103–133.

Ebbert, P.S., and R.D. Roe. 1998. Soil Erosion in the Palouse River Basin: Indications of Improvement. U.S. Geological Survey Fact Sheet FS-069-98

Eagleson, P.S. 1978. Climate, soil, and vegetation: 1. Introduction to water balance dynamics. Water Resources Research 14(5): 705–712.

Elsner, M.M., L. Cuo, N. Voisin, J.S. Deems, A.F. Hamlet, J.A. Vano, K.E.B. Mickelson, S.-Y. Lee, and D.P. Lettenmaier. 2010. Implications of 21st century climate change for the hydrology of Washington State. Climatic Change 102(1-2): 225–260.

Fuentes, J.P., M. Flury, D.R. Huggins, and D.F. Bezdicek. 2003. Soil water and nitrogen dynamics in dryland cropping systems of Washington State, USA. Soil and Tillage Research 71(1): 33–47.

Hupet, F., and M. Vanclooster. 2002. Intraseasonal dynamics of soil moisture variability within a small agricultural maize cropped field. Journal of Hydrology 261(1–4): 86–101.

Ibrahim, H.M., and D.R. Huggins. 2011. Spatio-temporal patterns of soil water storage under dryland agriculture at the watershed scale. Journal of Hydrology 404(3–4): 186–197.

Khakural, B.R., P.C. Robert, and D.R. Huggins. 1998. Use of non-contacting electromagnetic inductive method for estimating soil moisture across a landscape. Communications in Soil Science and Plant Analysis 29(11-14): 2055–2065.

Kilmer, V.J., and L.T. Alexander. 1949. Methods of making mechanical analyses of soils. Soil Science 68(1): 15–24.

Kornelsen, K.C., and P. Coulibaly. 2013. Advances in soil moisture retrieval from synthetic aperture radar and hydrological applications. Journal of Hydrology 476: 460–489.

Lafond, G.P., H. Loeppky, and D.A. Derksen. 1992. The effects of tillage systems and crop rotations on soil water conservation, seedling establishment and crop yield. Canadian Journal of Plant Science 72(1): 103–115.

Lesch, S.M., J.D. Rhoades, and D.L. Corwin. 2000. ESAP-95 Version 2.01 R: User manual and tutorial guide: Research Rpt. 146, USDA-ARS George E. Brown, Jr. Salinity Laboratory, Riverside, CA.

Machado, S., S. Petrie, K. Rhinhart, and R.E. Ramig. 2008. Tillage Effects on Water Use and Grain Yield of Winter Wheat and Green Pea in Rotation. Agronomy Journal 100(1): 154.

McNeill, J.D. 1980. Electromagnetic terrain conductivity measurement at low induction numbers, Tech. Note TN -6. Geonics Limited Mississauga, Ontario, Canada.

Mikhail, E.H., and G.P. Briner. 1978. Routine particle size analysis of soils using sodium hypochlorite and ultrasonic dispersion. Soil Research 16(2): 241–244.

Miller, P.R., R.E. Engel, and J.A. Holmes. 2006. Cropping Sequence Effect of Pea and Pea Management on Spring Wheat in the Northern Great Plains. Agronomy Journal 98(6): 1610.

Mohanty, B., and T. Skaggs. 2001. Spatio-temporal evolution and time-stable characteristics of soil moisture within remote sensing footprints with varying soil, slope, and vegetation. Advances in Water Resources 24(9–10): 1051–1067.

Papendick, R. I. 1987. Tillage and water conservation: experience in the Pacific Northwest. Soil Use and Management 3(2): 69–74.

Payne, W.A., P.E. Rasmussen, C. Chen, and R.E. Ramig. 2001. Assessing Simple Wheat and Pea Models Using Data from a Long-Term Tillage Experiment. Agronomy Journal 93(1): 250.

Qi, Z., P.N.S. Bartling, J.D. Jabro, A.W. Lenssen, W.M. Iversen, L.R. Ahuja, L. Ma, B.L. Allen, and R.G. Evans. 2013. Simulating Dryland Water Availability and Spring Wheat Production in the Northern Great Plains. Agronomy Journal 105(1): 37.

Qiu, H., D.R. Huggins, J.Q. Wu, M.E. Barber, D.K. Mccool, and S. Dun. 2011. Residue Management Impacts on Field-Scale Snow Distribution and Soil Water Storage. Transactions of the ASABE 54(5): 1639–1647.

Reedy, R.C., and B.R. Scanlon. 2003. Soil Water Content Monitoring Using Electromagnetic Induction. Journal of Geotechnical and Geoenvironmental Engineering 129(11): 1028–1039.

Rhoades, J.D., P. a. C. Raats, and R.J. Prather. 1976. Effects of Liquid-phase Electrical Conductivity, Water Content, and Surface Conductivity on Bulk Soil Electrical Conductivity. Soil Science Society of America Journal 40(5): 651–655.

Riar, D.S., D.A. Ball, J.P. Yenish, S.B. Wuest, and M.K. Corp. 2010. Comparison of Fallow Tillage Methods in the Intermediate Rainfall Inland Pacific Northwest. Agronomy Journal 102(6): 1664.

Robertson, E. 2010. Conservation tillage influences soil environmental conditions and carbon storage on a Palouse hillslope. M.S. Thesis, Soil and Land Resources-University of Idaho.

Robinson, D.A., H. Abdu, I. Lebron, and S.B. Jones. 2012. Imaging of hill-slope soil moisture wetting patterns in a semi-arid oak savanna catchment using time-lapse electromagnetic induction. Journal of Hydrology 416-417: 39–49.

Robinson, D.A., I. Lebron, B. Kocar, K. Phan, M. Sampson, N. Crook, and S. Fendorf. 2009. Time-lapse geophysical imaging of soil moisture dynamics in tropical deltaic soils:

An aid to interpreting hydrological and geochemical processes. Water Resources Research 45(4).

Sauer, D., S. Popp, A. Dittfurth, D. Altdorff, P. Dietrich, and H. Paasche. 2013. Soil Moisture Assessment over an Alpine Hillslope with Significant Soil Heterogeneity. Vadose Zone Journal 12(4).

Schillinger, W.F., and R.I. Papendick. 2008. Then and Now: 125 Years of Dryland Wheat Farming in the Inland Pacific Northwest. Agronomy Journal 100(Supplement_3): S–166.

Schwanghart, W., and N.J. Kuhn. 2010. TopoToolbox: A set of Matlab functions for topographic analysis. Environmental Modelling & Software 25(6): 770–781.

Seneviratne, S.I., T. Corti, E.L. Davin, M. Hirschi, E.B. Jaeger, I. Lehner, B. Orlowsky, and A.J. Teuling. 2010. Investigating soil moisture–climate interactions in a changing climate: A review. Earth-Science Reviews 99(3–4): 125–161.

Sheets, K.R., and J.M.H. Hendrickx. 1995. Noninvasive Soil Water Content Measurement Using Electromagnetic Induction. Water Resources Research 31(10): 2401–2409.

Singh, P., M. Flury, and W.F. Schillinger. 2011. Predicting seed-zone water content for summer fallow in the Inland Pacific Northwest, USA. Soil and Tillage Research 115–116: 94–104.

Soil Survey Staff. 2010. Keys to Soil Taxonomy. 11th ed. United States Department of Agriculture, Natural Resources Conservation Service, Washington, D.C.

Su, Z., J. Zhang, W. Wu, D. Cai, J. Lv, G. Jiang, J. Huang, J. Gao, R. Hartmann, and D. Gabriels. 2007. Effects of conservation tillage practices on winter wheat water-use efficiency and crop yield on the Loess Plateau, China. Agricultural Water Management 87(3): 307–314.

Sudduth, K.A., S.T. Drummond, and N.R. Kitchen. 2001. Accuracy issues in electromagnetic induction sensing of soil electrical conductivity for precision agriculture. Computers and Electronics in Agriculture 31(3): 239–264.

Tromp-van Meerveld, H.J., and J.J. McDonnell. 2009. Assessment of multi-frequency electromagnetic induction for determining soil moisture patterns at the hillslope scale. Journal of Hydrology 368(1–4): 56–67.

Van Wijk, W. Van, and D. De Vries. 1966. Periodic temperature variations in a homogeneous soil. Physics of Plant Environment, North-Holland Publ. Co., Amsterdam: 102–143.

Vereecken, H., J.A. Huisman, Y. Pachepsky, C. Montzka, J. van der Kruk, H. Bogena, L. Weihermüller, M. Herbst, G. Martinez, and J. Vanderborght. 2013. On the spatio-temporal dynamics of soil moisture at the field scale. Journal of Hydrology.

Wang, X., H. Xie, H. Guan, and X. Zhou. 2007. Different responses of MODIS-derived NDVI to root-zone soil moisture in semi-arid and humid regions. Journal of Hydrology 340(1–2): 12–24.

Western, A.W., G. Blöschl, and R.B. Grayson. 1998. Geostatistical characterisation of soil moisture patterns in the Tarrawarra catchment. Journal of Hydrology 205(1–2): 20–37.

Western, A.W., R.B. Grayson, and G. Blöschl. 2002. Scaling of soil moisture: A hydrologic perspective. Annual Review of Earth and Planetary Sciences 30(1): 149–180.

Western Regional Climate Center. 2012. Monthly Summary Data Lister. Available at http://www.wrcc.dri.edu/cgi-bin/cliMAIN.pl?id6152 (verified 28 August 2013).

Williams, J.D., and S.B. Wuest. 2011. Tillage and no-tillage conservation effectiveness in the intermediate precipitation zone of the inland Pacific Northwest, United States. Journal of Soil and Water Conservation 66(4): 242–249.

Wilson, D.J., A.W. Western, and R.B. Grayson. 2005. A terrain and data-based method for generating the spatial distribution of soil moisture. Advances in Water Resources 28(1): 43–54.

Zhu, Q., H. Lin, and J. Doolittle. 2010. Repeated Electromagnetic Induction Surveys for Determining Subsurface Hydrologic Dynamics in an Agricultural Landscape. Soil Science Society of America Journal 74(5): 1750.

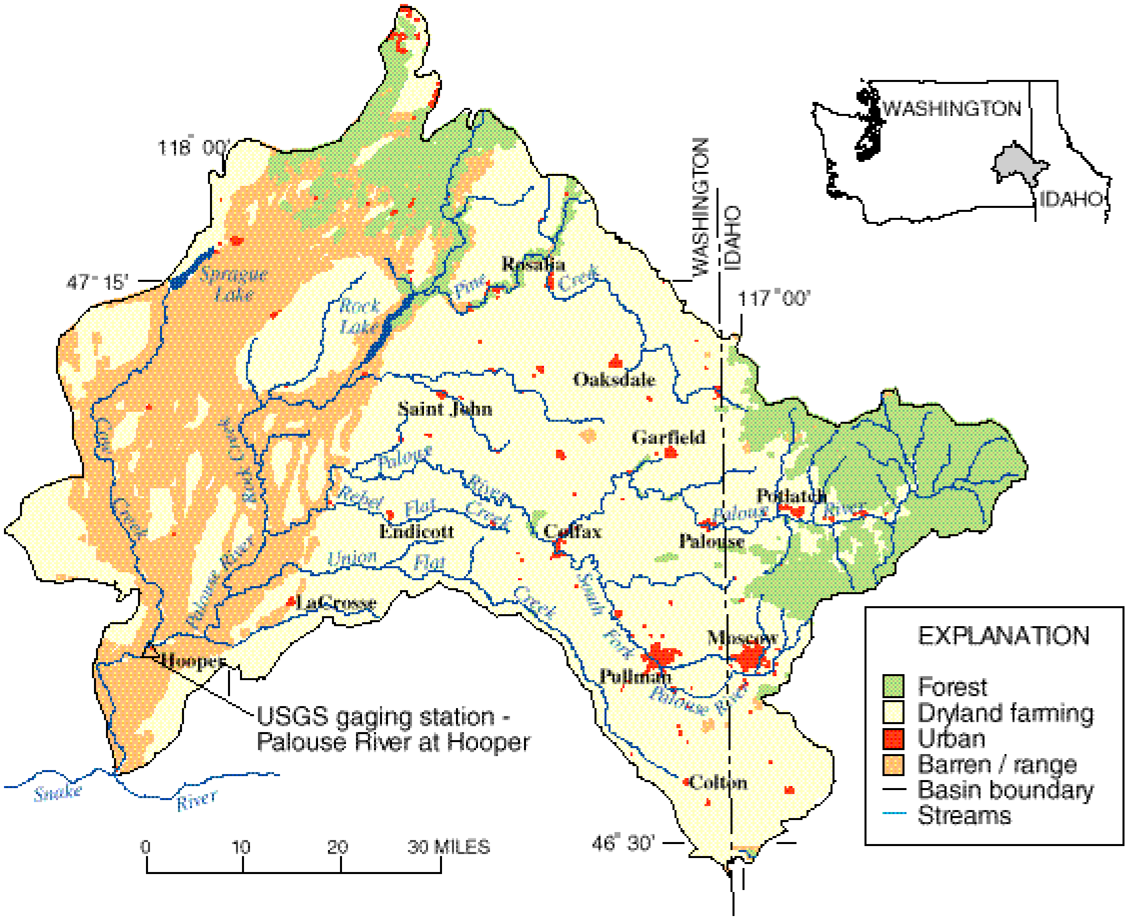

Figure 1. The Palouse area shown with its location in Idaho and Washington. Image from Ebbert and Roe, 1998.

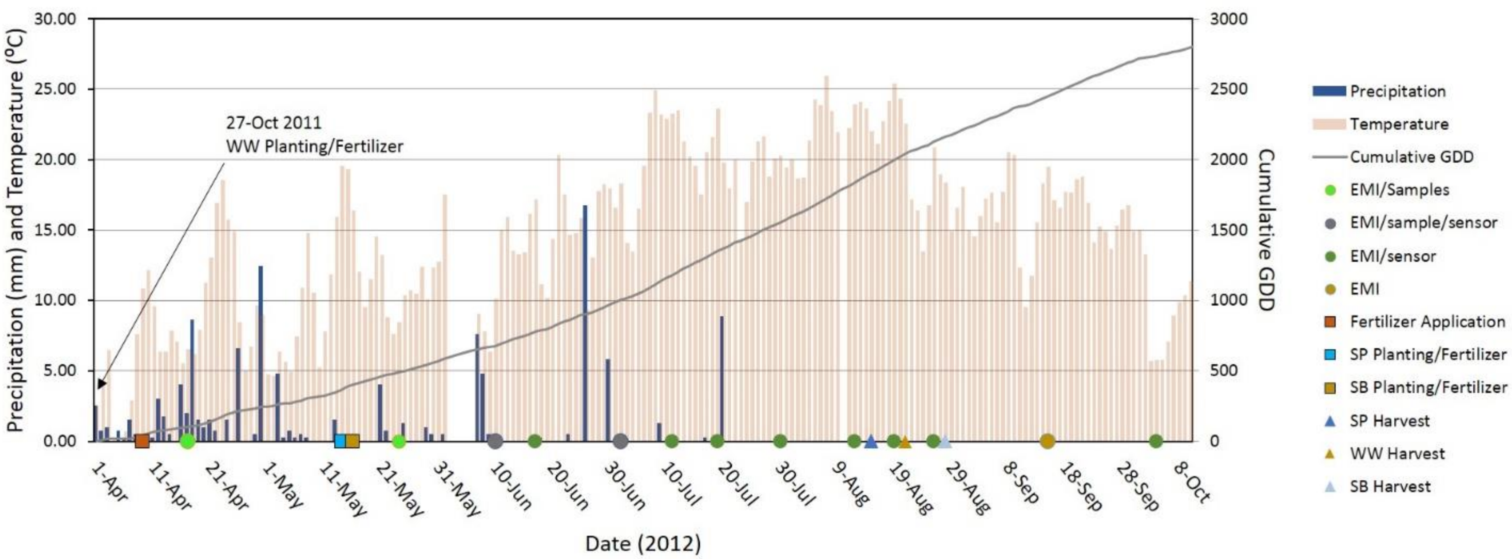

Figure 2. Temperature, precipitation, and growing degree days (GDD) plotted for the duration of the study. EMI/Samples represents dates that field scale apparent electrical conductivity with an electromagnetic induction (EMI) measuring device and soil samples were collected. EMI/Sample/Sensor represents dates that EMI, soil samples, and a soil moisture sensor were used to collect data. EMI/Sensor are dates that had data collection done using EMI and the soil moisture sensor. EMI represents dates that only field-scale EMI data was collected.

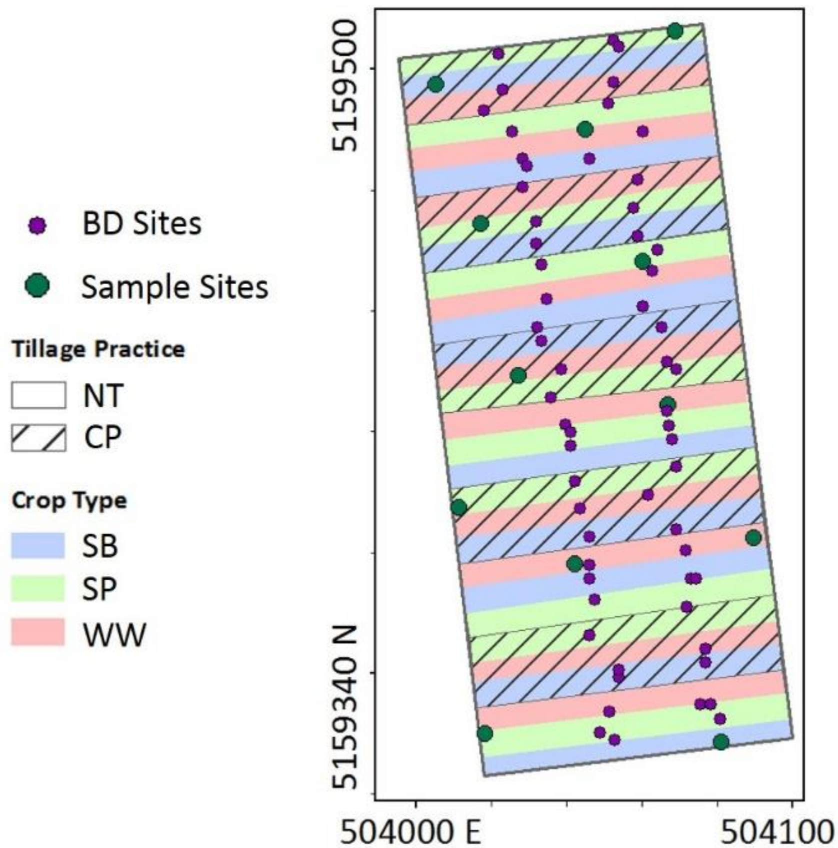

Figure 3. Bulk density (BD) and soil sampling sites with designated crop (spring barley (SB), spring pea (SP), and winter wheat (WW)) subplots and tillage plots (no till (NT) or chisel plow (CP)). Bulk density sites represent where samples were collected for bulk density determination. The samples sites marked are locations that soil samples and/or a soil moisture sensor were used to collect site specific data.

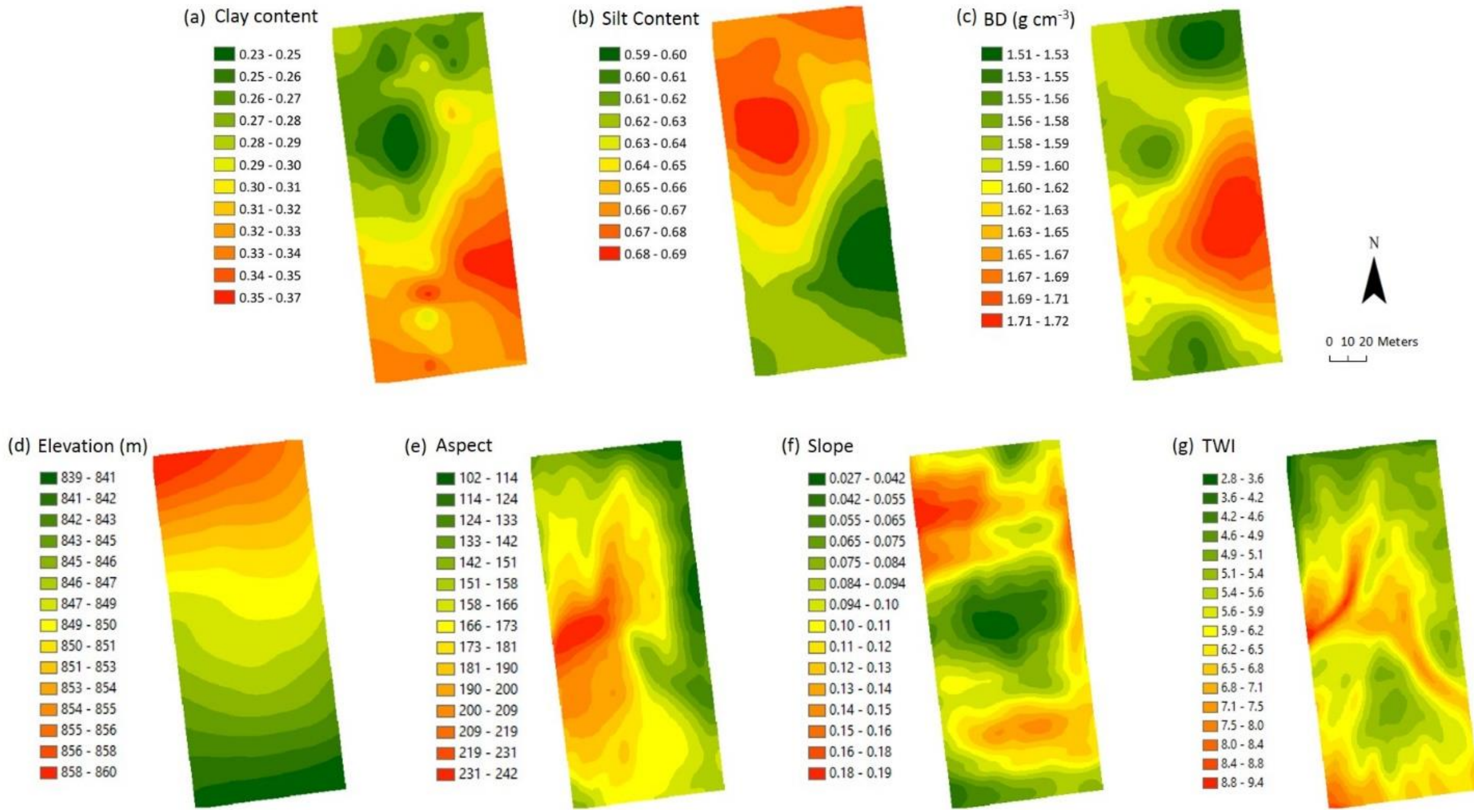

Figure 4. Predicted maps of (a – b) 43 clay and silt content (specified as fractions) samples to a depth of 100 cm and (c) 60 bulk density (BD) samples to a depth of 120 cm. Predicted distribution of the topographic features (d – g) elevation, aspect, slope, and topographic wetness index (TWI).

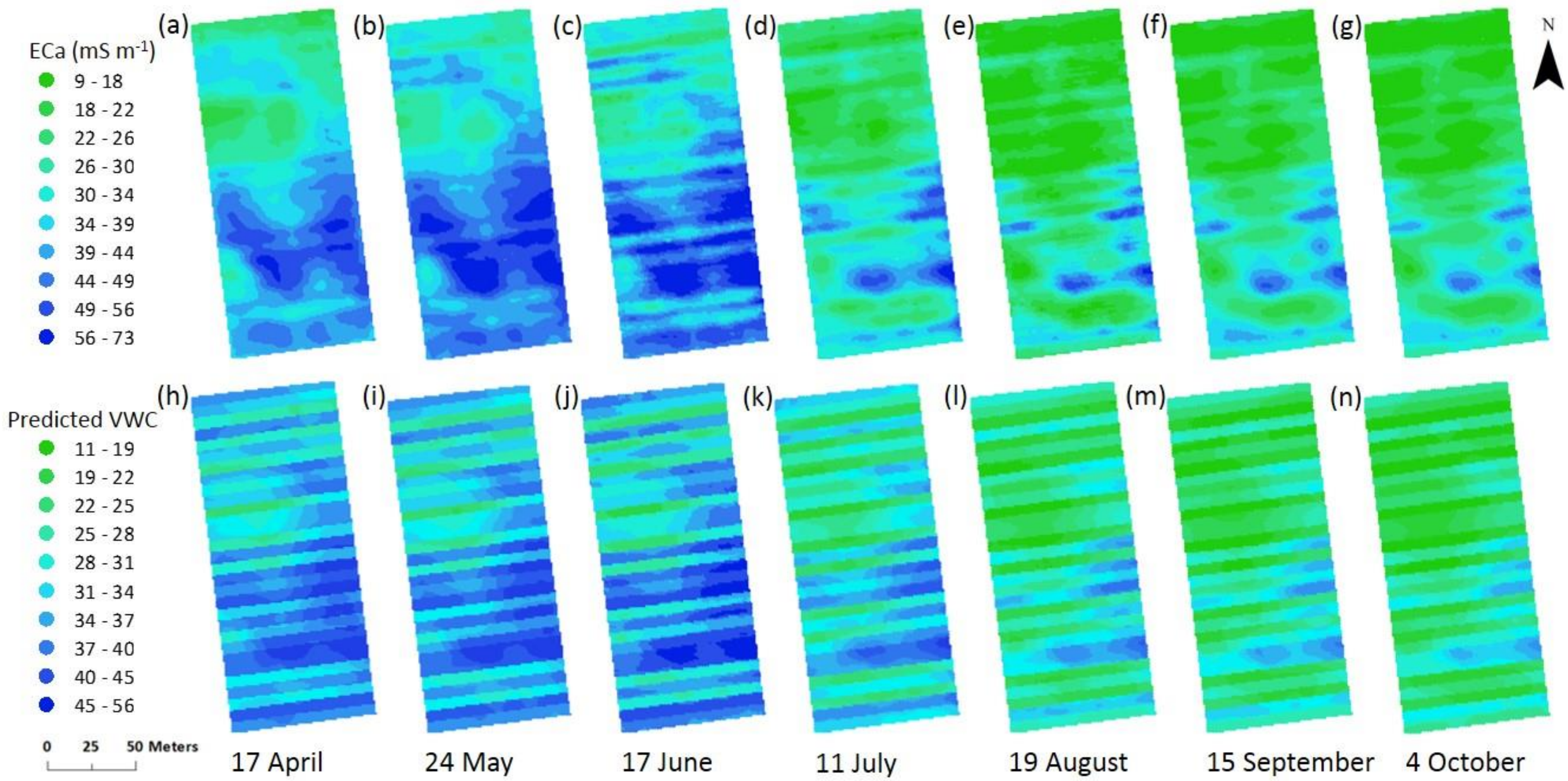

Figure 5. Predicted maps of (a) – (g) apparent electrical conductivity (EC_a) and (h) – (n) predicted volumetric water content (VWC) for the duration of the study.

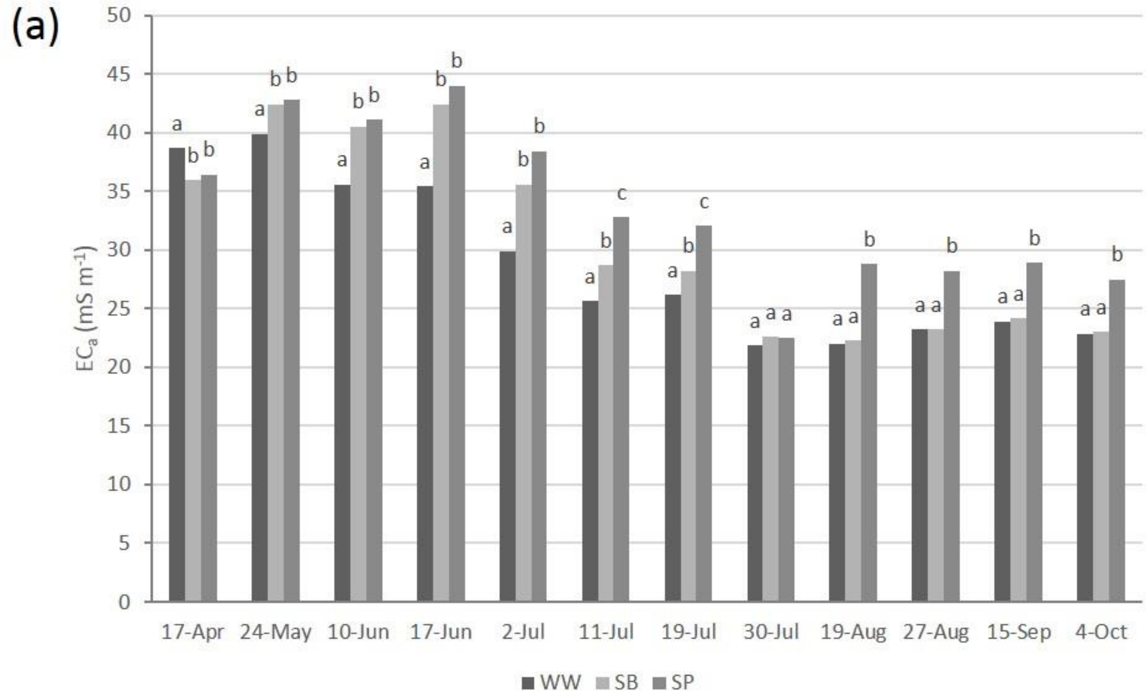

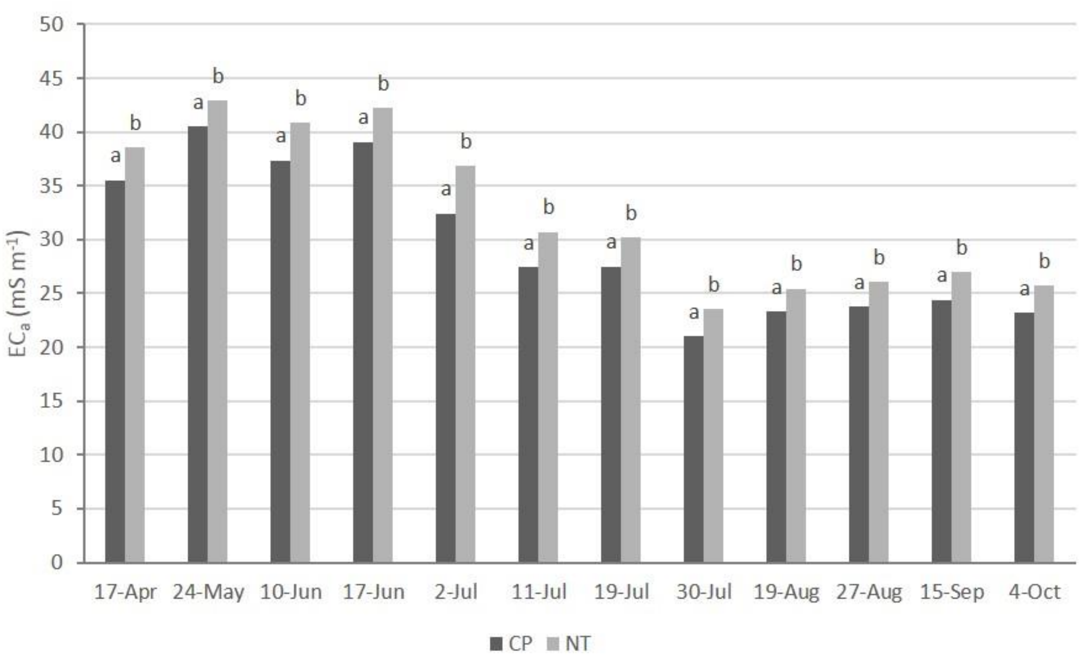

Figure 6. (a) Mean EC_a of winter wheat (WW), spring barley (SB), and spring pea (SP) subplots compared over the growing season. (b) Mean EC_a for chisel plow (CP) and no till (NT) plots are compared. Within date differences between crops or tillage practice are indicated by the lettering above columns (paired t-test, $\alpha < 0.05$).

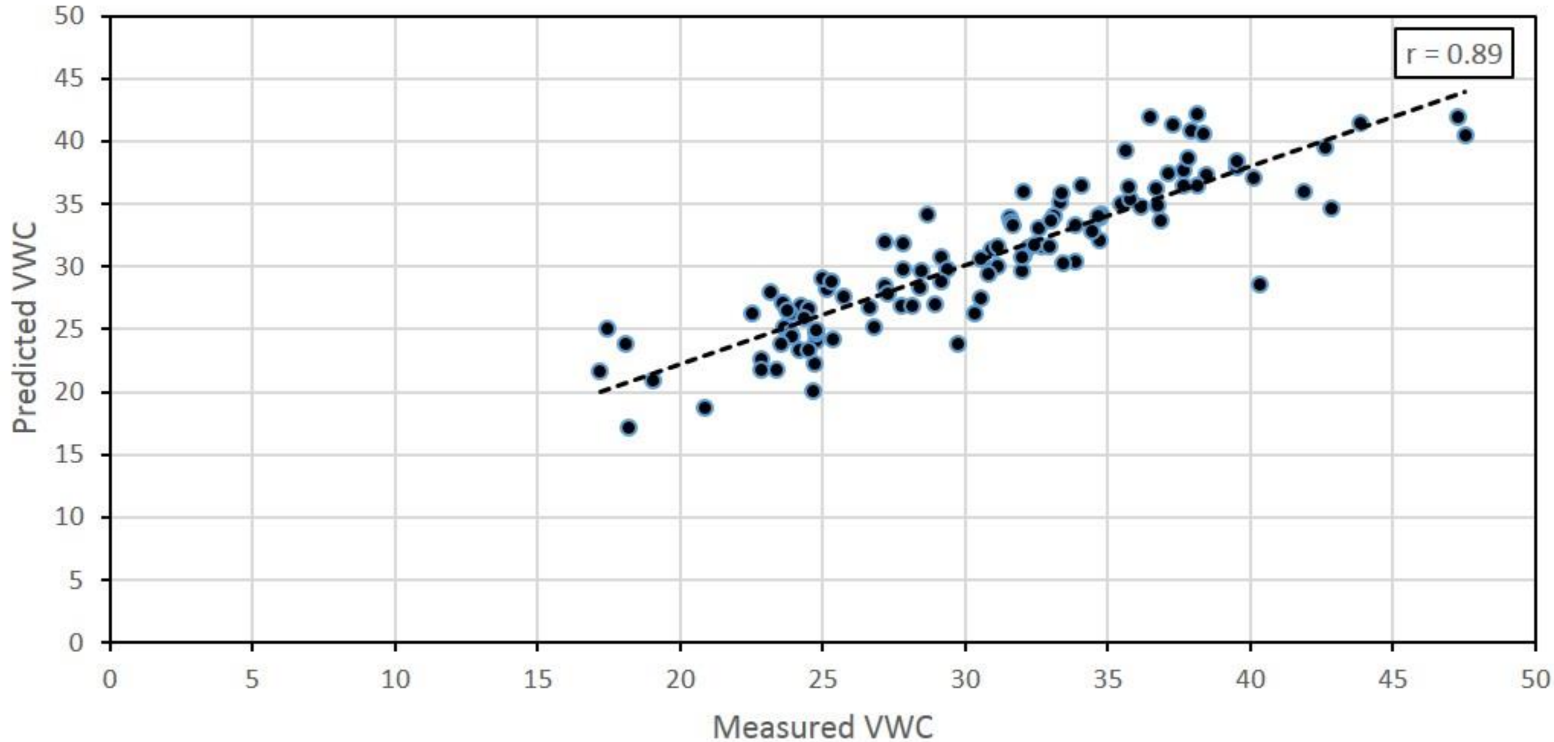

Figure 7. Predicted and measured volumetric water content (VWC) for the 12 sites from April to October, 2012 shown with the linear trendline and correlation coefficient (r).

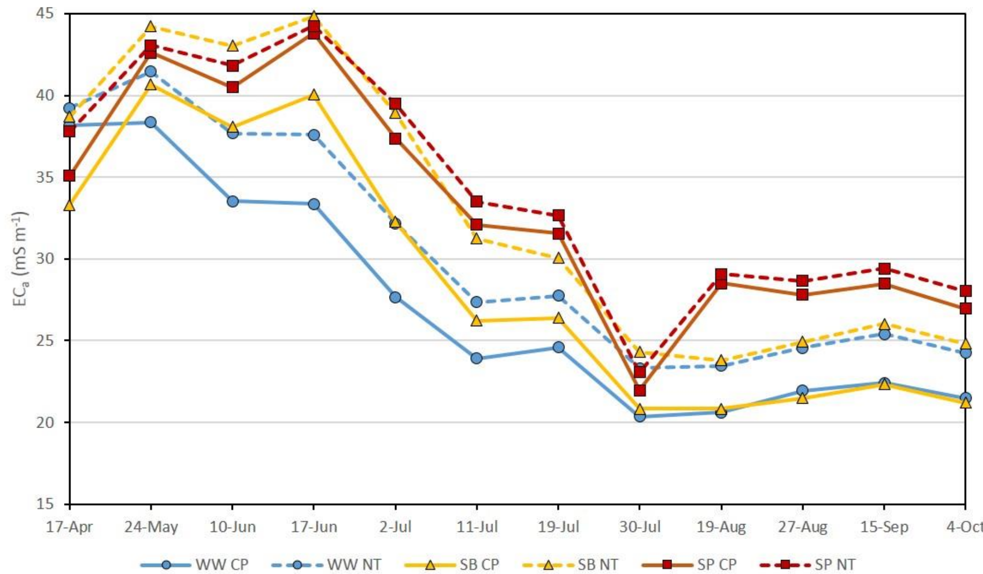

Figure 8. Mean EC_a of crop (winter wheat (WW), spring barley (SB), spring pea (SP)) and tillage (no till (NT), chisel plow (CP)) subplot combinations throughout the growing season. Significant differences between combinations are listed in Table 1.

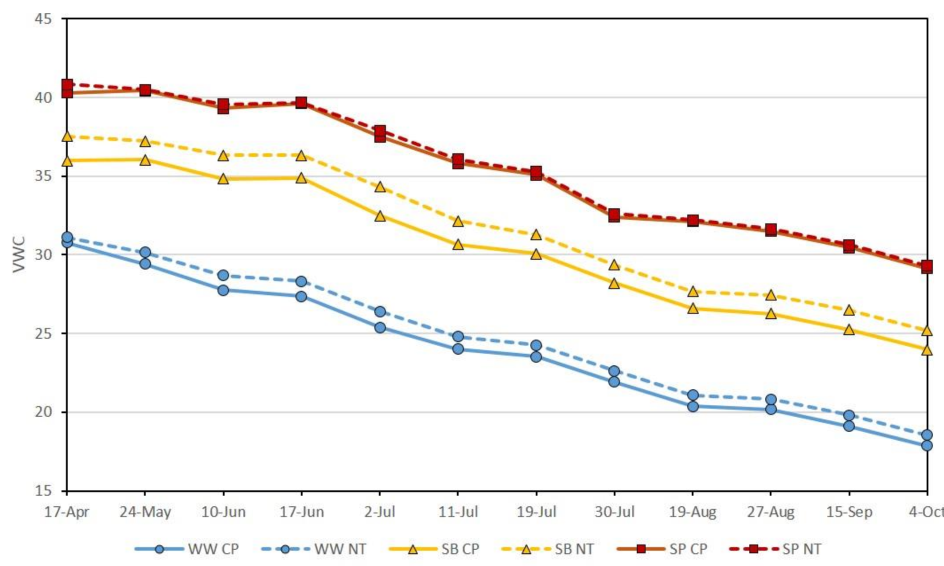

Figure 9. Predicted mean volumetric water content (VWC) for crop (winter wheat (WW), spring barley (SB), spring pea (SP)) and tillage (no till (NT), chisel plow (CP)) combinations. There were no significant differences between NT and CP for a specified crop and date.

Table 1. Summary statistics and variogram parameters for kriged variables (clay, silt, sand, bulk density (BD), and apparent electrical conductivity (EC_a) with date collected).

Variable	Date	Mean	Min	Max	Range	Sill	Nugget	Model Type
Clay Content	-	0.30	0.23	0.37	392.90	2.95	0.21	Spherical
Silt Content	-	0.64	0.58	0.71	392.90	3.03	0.20	Spherical
Sand Content	-	0.06	0.05	0.08	392.90	0.12	0.90	Spherical
BD (g cm^{-3})	-	1.61	1.43	1.77	137.14	0.96	0.39	Cubic
EC_a (mS m^{-1})	17-Apr	36.71	18.83	62.73	488.29	3.84	0.06	Cubic
EC_a (mS m^{-1})	24-May	41.58	23.03	69.92	314.19	2.48	0.07	Cubic
EC_a (mS m^{-1})	10-Jun	38.62	17.41	66.61	310.60	2.44	0.09	Cubic
EC_a (mS m^{-1})	17-Jun	40.97	16.55	72.57	464.17	3.65	1.11E-07	Cubic
EC_a (mS m^{-1})	2-Jul	35.02	8.45	76.70	395.30	3.52	0.27	Cubic
EC_a (mS m^{-1})	11-Jul	28.79	13.61	72.08	485.05	3.31	0.28	Cubic
EC_a (mS m^{-1})	19-Jul	28.47	13.62	75.06	428.44	3.28	0.44	Cubic
EC_a (mS m^{-1})	30-Jul	22.39	5.22	58.51	486.39	4.47	3.16E-07	Cubic
EC_a (mS m^{-1})	19-Aug	24.26	6.21	65.80	454.08	3.12	6.23E-08	Cubic
EC_a (mS m^{-1})	27-Aug	24.39	10.06	60.79	422.94	3.39	0.38	Cubic
EC_a (mS m^{-1})	15-Sep	25.51	11.52	59.77	418.70	3.51	0.33	Cubic
EC_a (mS m^{-1})	4-Oct	24.25	11.92	58.18	418.80	3.50	0.32	Cubic

Table 2. A correlation matrix of growing degree days (GDD), elevation, aspect, slope, topographic wetness index (TWI), sand, silt, and clay content (as a fraction), electrical conductivity (EC_a), bulk density (BD), and volumetric water content (VWC) is shown. The values indicate the correlation coefficient (r) between two variables.

Variable	GDD	Elevation (m)	Aspect	Slope	TWI	Sand	Silt	Clay	EC_a (mS m^{-1})	BD (g cm^{-3})	VWC
GDD	1.000										
Elevation (m)	0.031	1.000									
Aspect	-0.034	-0.230	1.000								
Slope	0.088	0.495	-0.201	1.000							
TWI	-0.052	-0.689	0.411	-0.604	1.000						
Sand	-0.038	0.195	0.439	-0.201	-0.098	1.000					
Silt	-0.019	0.762	-0.127	0.269	-0.438	0.426	1.000				
Clay	0.023	-0.735	0.049	-0.218	0.419	-0.549	-0.990	1.000			
EC_a (mS m^{-1})	-0.477	-0.629	0.185	-0.215	0.295	-0.152	-0.680	0.652	1.000		
BD (g cm^{-3})	0.031	-0.324	0.211	-0.080	0.224	0.001	-0.687	0.635	0.398	1.000	
VWC	-0.594	-0.338	-0.123	-0.055	0.120	0.006	-0.197	0.181	0.601	0.069	1.000

Table 3. The measured variables (MVs) and their corresponding influence on the Condensed Variable (CV). The larger the absolute value, the greater the influence the MV has on that CV. Above the MVs is the cumulative variance for each CV. This represents the amount of variance in the data that is accounted for by the corresponding CV.

MV	CV1	CV2	CV3
GDD	0.09	0.87	-0.05
Elevation	0.48	-0.11	0.85
Silt	0.53	-0.19	-0.34
Clay	-0.52	0.20	0.41
EC_a	-0.46	-0.38	0.02
Axis Variance	0.65	0.24	0.06
Σ Variance	0.65	0.89	0.96

Table 4. Mean average EC_a ($mS\ m^{-1}$) for winter wheat (WW), spring barley (SB), and spring pea (SP) chisel plow (CP) and no till (NT) subplots throughout the growing season are shown. * indicates EC_a of NT and CP of crop subplots on the specified dates were significantly different.

WW	17-Apr	24-May	10-Jun*	17-Jun	2-Jul*	11-Jul*	19-Jul*	30-Jul*	19-Aug*	27-Aug	15-Sep*	4-Oct
CP mean	38.16	38.36	33.52	33.36	27.66	23.91	24.60	20.36	20.60	21.93	22.43	21.48
NT mean	39.23	41.46	37.67	37.59	32.17	27.35	27.76	23.33	23.47	24.56	25.42	24.26

SB	17-Apr*	24-May	10-Jun	17-Jun	2-Jul	11-Jul*	19-Jul	30-Jul	19-Aug	27-Aug	15-Sep	4-Oct
CP mean	33.31	40.66	38.07	40.04	32.27	26.23	26.38	20.84	20.84	21.49	22.33	21.21
NT mean	38.69	44.23	43.03	44.83	38.93	31.24	30.07	24.30	23.79	24.93	26.04	24.80

SP	17-Apr	24-May	10-Jun	17-Jun	2-Jul	11-Jul	19-Jul	30-Jul	19-Aug	27-Aug	15-Sep	4-Oct
CP mean	35.07	42.62	40.50	43.81	37.37	32.10	31.56	21.97	28.51	27.80	28.47	26.95
NT mean	37.79	43.06	41.82	44.24	39.49	33.51	32.65	23.07	29.08	28.65	29.43	28.04

Appendices

Appendix A. Site Locations with Crop and Tillage Type

Site	x	y	Tillage	Crop
1	504079.80	5159316.00	No	Barley
2	504017.00	5159318.00	No	Pea
3	504040.90	5159363.00	No	Wheat
4	504088.40	5159370.00	No	Wheat
5	504008.10	5159378.00	Yes	Pea
6	504065.50	5159405.00	No	Wheat
7	504025.90	5159413.00	Yes	Wheat
8	504058.90	5159443.00	No	Pea
9	504015.90	5159453.00	Yes	Pea
10	504043.80	5159478.00	No	Wheat
11	504004.00	5159490.00	Yes	Barley
12	504067.60	5159506.00	Yes	Pea

Appendix B. Data Inputted into Correlation Matrix and Principal Component Analysis

Day of Year	GDD	Site	Elevation (m)	Aspect	Slope	TWI	Sand	Silt	Clay	VWC	EC_a (mS m^{-1})	BD (g cm^{-3})
108	102.96	1	839.39	158.64	0.087	6.61	0.048	0.624	0.328	39.56	30.08	1.58
108	102.96	2	840.60	153.84	0.050	7.74	0.052	0.614	0.334	47.27	28.21	1.58
108	102.96	3	845.36	193.28	0.105	5.29	0.050	0.602	0.348	39.55	42.40	1.63
108	102.96	4	844.24	128.31	0.116	6.32	0.046	0.582	0.371	42.64	40.32	1.69
108	102.96	5	845.55	214.37	0.099	5.60	0.063	0.626	0.311	36.48	30.16	1.64
108	102.96	6	848.27	167.47	0.058	6.13	0.058	0.613	0.329	42.85	32.62	1.72
108	102.96	7	848.22	223.63	0.046	7.61	0.060	0.656	0.284	40.34	25.54	1.59
108	102.96	8	850.72	173.14	0.095	6.09	0.056	0.657	0.287	37.66	20.94	1.62
108	102.96	9	852.18	169.71	0.135	5.88	0.058	0.679	0.263	36.17	17.25	1.58
108	102.96	10	854.79	173.49	0.115	5.67	0.049	0.653	0.298	33.85	24.69	1.55
108	102.96	11	858.38	148.70	0.123	4.76	0.050	0.665	0.285	33.35	20.83	1.59
108	102.96	12	855.13	102.43	0.097	3.73	0.057	0.679	0.264	36.78	15.42	1.54
145	488.89	1	839.39	158.64	0.087	6.61	0.048	0.624	0.328	38.47	33.53	1.58
145	488.89	2	840.60	153.84	0.050	7.74	0.052	0.614	0.334	43.87	31.90	1.58
145	488.89	5	845.55	214.37	0.099	5.60	0.063	0.626	0.311	38.15	36.36	1.64
145	488.89	8	850.72	173.14	0.095	6.09	0.056	0.657	0.287	40.14	24.26	1.62
145	488.89	12	855.13	102.43	0.097	3.73	0.057	0.679	0.264	35.50	21.19	1.54
162	677.68	1	839.39	158.64	0.087	6.61	0.048	0.624	0.328	38.14	33.16	1.58
162	677.68	2	840.60	153.84	0.050	7.74	0.052	0.614	0.334	47.54	31.29	1.58
162	677.68	5	845.55	214.37	0.099	5.60	0.063	0.626	0.311	37.93	34.38	1.64
162	677.68	8	850.72	173.14	0.095	6.09	0.056	0.657	0.287	41.91	23.24	1.62
162	677.68	9	852.18	169.71	0.135	5.88	0.058	0.679	0.263	33.87	20.02	1.58
162	677.68	12	855.13	102.43	0.097	3.73	0.057	0.679	0.264	36.87	19.10	1.54
169	776.25	1	839.39	158.64	0.087	6.61	0.048	0.624	0.328	37.65	34.63	1.58
169	776.25	2	840.60	153.84	0.050	7.74	0.052	0.614	0.334	38.38	32.83	1.58
169	776.25	3	845.36	193.28	0.105	5.29	0.050	0.602	0.348	28.68	37.47	1.63
169	776.25	4	844.24	128.31	0.116	6.32	0.046	0.582	0.371	33.41	37.67	1.69
169	776.25	5	845.55	214.37	0.099	5.60	0.063	0.626	0.311	37.31	37.42	1.64
169	776.25	6	848.27	167.47	0.058	6.13	0.058	0.613	0.329	27.81	32.38	1.72
169	776.25	7	848.22	223.63	0.046	7.61	0.060	0.656	0.284	17.48	22.94	1.59
169	776.25	8	850.72	173.14	0.095	6.09	0.056	0.657	0.287	36.70	25.16	1.62
169	776.25	9	852.18	169.71	0.135	5.88	0.058	0.679	0.263	32.60	20.50	1.58
169	776.25	10	854.79	173.49	0.115	5.67	0.049	0.653	0.298	25.14	26.86	1.55
169	776.25	11	858.38	148.70	0.123	4.76	0.050	0.665	0.285	34.75	26.17	1.59
169	776.25	12	855.13	102.43	0.097	3.73	0.057	0.679	0.264	33.13	21.88	1.54
184	1005.16	1	839.39	158.64	0.087	6.61	0.048	0.624	0.328	35.82	33.98	1.58
184	1005.16	2	840.60	153.84	0.050	7.74	0.052	0.614	0.334	35.62	31.75	1.58
184	1005.16	3	845.36	193.28	0.105	5.29	0.050	0.602	0.348	27.17	33.18	1.63
184	1005.16	4	844.24	128.31	0.116	6.32	0.046	0.582	0.371	33.00	33.44	1.69
184	1005.16	5	845.55	214.37	0.099	5.60	0.063	0.626	0.311	37.83	31.61	1.64
184	1005.16	6	848.27	167.47	0.058	6.13	0.058	0.613	0.329	28.49	28.37	1.72
184	1005.16	7	848.22	223.63	0.046	7.61	0.060	0.656	0.284	18.12	22.10	1.59
184	1005.16	8	850.72	173.14	0.095	6.09	0.056	0.657	0.287	34.81	21.44	1.62
184	1005.16	9	852.18	169.71	0.135	5.88	0.058	0.679	0.263	32.21	18.18	1.58
184	1005.16	10	854.79	173.49	0.115	5.67	0.049	0.653	0.298	25.35	16.41	1.55
184	1005.16	11	858.38	148.70	0.123	4.76	0.050	0.665	0.285	32.02	14.90	1.59
184	1005.16	12	855.13	102.43	0.097	3.73	0.057	0.679	0.264	32.67	16.75	1.54
193	1178.45	1	839.39	158.64	0.087	6.61	0.048	0.624	0.328	30.92	23.13	1.58

193	1178.45	2	840.60	153.84	0.050	7.74	0.052	0.614	0.334	34.07	24.63	1.58
193	1178.45	3	845.36	193.28	0.105	5.29	0.050	0.602	0.348	24.97	25.78	1.63
193	1178.45	4	844.24	128.31	0.116	6.32	0.046	0.582	0.371	32.07	26.39	1.69
193	1178.45	5	845.55	214.37	0.099	5.60	0.063	0.626	0.311	37.11	29.79	1.64
193	1178.45	6	848.27	167.47	0.058	6.13	0.058	0.613	0.329	25.73	23.40	1.72
193	1178.45	7	848.22	223.63	0.046	7.61	0.060	0.656	0.284	17.19	17.30	1.59
193	1178.45	8	850.72	173.14	0.095	6.09	0.056	0.657	0.287	32.97	15.12	1.62
193	1178.45	9	852.18	169.71	0.135	5.88	0.058	0.679	0.263	30.89	14.89	1.58
193	1178.45	10	854.79	173.49	0.115	5.67	0.049	0.653	0.298	24.75	18.51	1.55
193	1178.45	11	858.38	148.70	0.123	4.76	0.050	0.665	0.285	27.84	17.65	1.59
193	1178.45	12	855.13	102.43	0.097	3.73	0.057	0.679	0.264	32.42	19.37	1.54
201	1348.79	1	839.39	158.64	0.087	6.61	0.048	0.624	0.328	29.15	23.32	1.58
201	1348.79	2	840.60	153.84	0.050	7.74	0.052	0.614	0.334	32.08	25.12	1.58
201	1348.79	3	845.36	193.28	0.105	5.29	0.050	0.602	0.348	23.16	24.42	1.63
201	1348.79	4	844.24	128.31	0.116	6.32	0.046	0.582	0.371	31.14	25.68	1.69
201	1348.79	5	845.55	214.37	0.099	5.60	0.063	0.626	0.311	35.75	28.75	1.64
201	1348.79	6	848.27	167.47	0.058	6.13	0.058	0.613	0.329	22.53	21.49	1.72
201	1348.79	7	848.22	223.63	0.046	7.61	0.060	0.656	0.284	19.05	17.13	1.59
201	1348.79	8	850.72	173.14	0.095	6.09	0.056	0.657	0.287	31.15	17.62	1.62
201	1348.79	9	852.18	169.71	0.135	5.88	0.058	0.679	0.263	29.37	17.41	1.58
201	1348.79	10	854.79	173.49	0.115	5.67	0.049	0.653	0.298	24.18	18.09	1.55
201	1348.79	11	858.38	148.70	0.123	4.76	0.050	0.665	0.285	25.30	16.74	1.59
201	1348.79	12	855.13	102.43	0.097	3.73	0.057	0.679	0.264	30.57	18.16	1.54
212	1555.15	1	839.39	158.64	0.087	6.61	0.048	0.624	0.328	28.43	17.78	1.58
212	1555.15	2	840.60	153.84	0.050	7.74	0.052	0.614	0.334	31.59	21.16	1.58
212	1555.15	3	845.36	193.28	0.105	5.29	0.050	0.602	0.348	24.26	23.56	1.63
212	1555.15	4	844.24	128.31	0.116	6.32	0.046	0.582	0.371	30.81	26.43	1.69
212	1555.15	5	845.55	214.37	0.099	5.60	0.063	0.626	0.311	34.68	23.37	1.64
212	1555.15	6	848.27	167.47	0.058	6.13	0.058	0.613	0.329	24.77	18.84	1.72
212	1555.15	7	848.22	223.63	0.046	7.61	0.060	0.656	0.284	20.90	12.28	1.59
212	1555.15	8	850.72	173.14	0.095	6.09	0.056	0.657	0.287	29.14	10.70	1.62
212	1555.15	9	852.18	169.71	0.135	5.88	0.058	0.679	0.263	27.79	10.33	1.58
212	1555.15	10	854.79	173.49	0.115	5.67	0.049	0.653	0.298	23.41	15.78	1.55
212	1555.15	11	858.38	148.70	0.123	4.76	0.050	0.665	0.285	23.89	10.80	1.59
212	1555.15	12	855.13	102.43	0.097	3.73	0.057	0.679	0.264	26.63	7.80	1.54
232	1994.90	1	839.39	158.64	0.087	6.61	0.048	0.624	0.328	28.94	19.21	1.58
232	1994.90	2	840.60	153.84	0.050	7.74	0.052	0.614	0.334	31.65	25.69	1.58
232	1994.90	3	845.36	193.28	0.105	5.29	0.050	0.602	0.348	24.79	23.13	1.63
232	1994.90	4	844.24	128.31	0.116	6.32	0.046	0.582	0.371	30.58	25.80	1.69
232	1994.90	5	845.55	214.37	0.099	5.60	0.063	0.626	0.311	34.72	23.01	1.64
232	1994.90	6	848.27	167.47	0.058	6.13	0.058	0.613	0.329	22.84	17.70	1.72
232	1994.90	7	848.22	223.63	0.046	7.61	0.060	0.656	0.284	18.20	12.94	1.59
232	1994.90	8	850.72	173.14	0.095	6.09	0.056	0.657	0.287	27.19	15.60	1.62
232	1994.90	9	852.18	169.71	0.135	5.88	0.058	0.679	0.263	24.53	15.25	1.58
232	1994.90	10	854.79	173.49	0.115	5.67	0.049	0.653	0.298	24.66	15.71	1.55
232	1994.90	11	858.38	148.70	0.123	4.76	0.050	0.665	0.285	23.68	13.04	1.59
232	1994.90	12	855.13	102.43	0.097	3.73	0.057	0.679	0.264	23.61	14.91	1.54
239	2126.00	1	839.39	158.64	0.087	6.61	0.048	0.624	0.328	28.17	20.69	1.58
239	2126.00	2	840.60	153.84	0.050	7.74	0.052	0.614	0.334	31.66	26.81	1.58
239	2126.00	3	845.36	193.28	0.105	5.29	0.050	0.602	0.348	23.88	24.12	1.63
239	2126.00	4	844.24	128.31	0.116	6.32	0.046	0.582	0.371	30.33	23.41	1.69

239	2126.00	5	845.55	214.37	0.099	5.60	0.063	0.626	0.311	34.46	27.13	1.64
239	2126.00	8	850.72	173.14	0.095	6.09	0.056	0.657	0.287	27.28	15.20	1.62
239	2126.00	9	852.18	169.71	0.135	5.88	0.058	0.679	0.263	24.37	14.85	1.58
239	2126.00	11	858.38	148.70	0.123	4.76	0.050	0.665	0.285	23.90	12.33	1.59
239	2126.00	12	855.13	102.43	0.097	3.73	0.057	0.679	0.264	23.75	14.85	1.54
278	2738.33	2	840.60	153.84	0.050	7.74	0.052	0.614	0.334	32.00	26.53	1.58
278	2738.33	3	845.36	193.28	0.105	5.29	0.050	0.602	0.348	24.71	23.86	1.63
278	2738.33	4	844.24	128.31	0.116	6.32	0.046	0.582	0.371	29.75	23.42	1.69
278	2738.33	5	845.55	214.37	0.099	5.60	0.063	0.626	0.311	33.43	26.86	1.64
278	2738.33	8	850.72	173.14	0.095	6.09	0.056	0.657	0.287	26.81	14.55	1.62
278	2738.33	9	852.18	169.71	0.135	5.88	0.058	0.679	0.263	24.51	14.18	1.58
278	2738.33	11	858.38	148.70	0.123	4.76	0.050	0.665	0.285	22.88	11.81	1.59
278	2738.33	12	855.13	102.43	0.097	3.73	0.057	0.679	0.264	23.56	14.01	1.54

Appendix C. Weather Data

Day of year	GDD	Average Temperature (^oC)	Max Temperature (^oC)	Min Temperature (^oC)
92	3.2155	2.557	6.118	0.313
93	7.337	3.88	8.63	-0.387
94	15.409	6.475	15.76	0.384
95	15.7745	0.167	3.942	-3.211
96	15.871	-0.032	3.37	-3.177
97	17.7985	0.671	5.485	-1.63
98	21.165	2.916	9.87	-3.137
99	29.2585	7.59	16.14	0.047
100	40.1495	10.82	17.64	4.142
101	53.6015	12.18	20.45	6.454
102	63.6705	9.56	16.13	4.008
103	70.6565	6.362	12.68	1.292
104	77.399	6.346	12.36	1.125
105	84.455	7.85	13.06	1.052
106	91.7655	7.06	11.92	2.701
107	96.697	5.542	7.9	1.963
108	102.9575	6.527	11.84	0.681
109	109.6575	6.162	10.67	2.73
110	116.139	7.94	12.41	0.553
111	127.254	11.25	13.32	8.91
112	140.2725	13.07	19.48	6.557
113	157.3275	16.93	26.51	7.6
114	175.1975	18.54	25.16	10.58
115	190.6475	15.72	20.69	10.21
116	205.6775	14.92	22.13	7.93
117	213.4225	8.45	12.12	3.37
118	218.8185	4.973	9.1	1.692
119	224.668	6.742	10.54	1.159
120	234.3265	9.64	16.81	2.507
121	243.0085	8.99	13.26	4.104
122	247.952	4.763	8.33	1.557
123	253.1905	4.606	10.77	-0.293
124	260.937	6.375	12.52	2.973
125	266.117	5.635	7.96	2.4
126	271.4835	4.954	9.27	1.463
127	278.44	7.41	14.53	-0.617
128	288.2915	10.9	18.51	1.193
129	301.9315	14.76	23	4.28
130	311.0565	10.55	14.31	3.94
131	315.8295	5.203	10.37	-0.824
132	322.509	7.8	15.22	-1.861
133	333.4535	11.85	20.12	1.769
134	348.3475	15.93	25.57	4.218
135	367.0775	19.58	28.35	9.11
136	385.7825	19.35	26.48	10.93
137	402.0875	16.38	20.99	11.62
138	413.495	12.03	16.09	6.725
139	422.6275	9.5	14.76	3.505
140	433.3485	11.5	18.51	2.932
141	448.0885	14.52	21.15	8.33

142	462.6535	13.23	19.12	10.01
143	471.489	8.82	12.22	5.451
144	479.8855	7.59	12.42	4.373
145	488.886	8.47	14.53	3.471
146	498.8635	10.34	15.71	4.245
147	509.1235	10.74	15.2	5.32
148	520.301	10.47	16.37	5.985
149	532.428	12.41	19.38	4.874
150	542.617	10.06	14.46	5.918
151	554.967	12.31	17.67	7.03
152	566.937	12.78	16.48	7.46
153	584.642	17.52	24	11.41
159	653.0885	9.07	15.74	2.064
160	661.1055	7.78	12.32	3.714
161	666.5045	6.348	8.43	2.368
162	677.6825	10.15	16.07	6.286
163	692.2395	15	22.49	6.624
164	707.3145	15.89	21.82	8.33
165	720.7395	13.52	17.84	9.01
166	733.0185	13.3	19.14	5.418
167	745.447	13.4	19.44	5.417
168	760.355	16.15	24.23	5.586
169	776.25	17.19	21.35	10.44
170	786.8755	11.13	14.7	6.551
171	796.878	10.16	15.26	4.745
172	809.593	14.34	22.33	3.1
173	829.623	20.35	29.08	10.98
174	846.623	17.54	22.86	11.14
175	862.533	14.69	21.31	10.51
176	877.408	14.76	20.04	9.71
177	893.423	15.88	22.02	10.01
178	903.1465	9.36	13.56	5.887
179	915.3565	13.05	20.14	4.28
180	932.8865	17.76	26.93	8.13
181	951.0565	18.25	23.62	12.72
182	970.6715	17.97	26.3	12.93
183	986.9365	16.56	21.52	11.01
184	1005.1615	18.33	25.73	10.72
185	1017.3235	14.07	17.87	6.454
186	1030.019	13.5	21.55	3.841
187	1044.71	16.54	23.09	6.292
188	1063.55	19.54	29.21	8.47
189	1086.32	23.33	32.38	13.16
190	1110.385	24.94	33.86	14.27
191	1133.39	23.2	28.83	17.18
192	1156.135	22.89	29.28	16.21
193	1178.445	23.26	29.68	14.94
194	1202.24	23.52	32.72	14.87
195	1224.025	21.3	27.83	15.74
196	1244.2	20.19	25.08	15.27
197	1263.545	19.57	25.64	13.05

198	1282.135	17.55	26.23	10.95
199	1304.02	20.49	29.31	14.46
200	1325.335	21.61	28.13	14.5
201	1348.79	23.64	32.48	14.43
202	1369.585	19.8	27.56	14.03
203	1386.855	17.92	24.69	9.85
204	1407.07	20.06	28.57	11.86
205	1421.305	14.33	20.91	7.56
206	1437.3025	16.98	25.03	6.965
207	1456.1375	19.89	29.14	8.53
208	1477.6075	21.28	29.98	12.96
209	1498.2725	21.65	28.54	12.79
210	1516.6425	18.79	26.47	10.27
211	1534.7375	20.1	28.5	7.69
212	1555.1525	20.28	27.84	12.99
213	1573.8725	19.47	27.73	9.71
214	1592.3925	20.03	28.61	8.43
215	1610.4525	18.68	25.64	10.48
216	1628.6425	18.73	26.21	10.17
217	1649.3925	21.34	30.99	10.51
218	1673.2575	24.3	34.36	13.37
219	1696.9475	23.86	32.59	14.79
220	1722.7675	25.96	35.67	15.97
221	1745.0975	23.42	30.29	14.37
222	1766.8475	21.98	32.55	10.95
224	1811.871	22.25	31.59	12.2
225	1835.416	23.92	33.99	13.1
226	1858.996	24.08	33.89	13.27
227	1881.531	23.65	31.75	13.32
228	1903.806	22.04	30.02	14.53
229	1924.576	21.11	29.41	12.13
230	1945.766	22.75	32.33	10.05
231	1970.151	24.16	34.7	14.07
232	1994.901	25.39	34.33	15.17
233	2019.211	24.33	33.02	15.6
234	2042.136	22.52	29.34	16.51
235	2059.306	17.19	24.16	10.18
236	2074.5135	16.42	23.49	6.925
237	2088.2785	13.5	20.04	7.49
238	2104.504	16.75	27.37	5.081
239	2126.004	20.85	31.32	11.68
240	2144.409	18.99	26.36	10.45
241	2161.914	18.37	26.21	8.8
242	2176.884	14.91	20.71	9.23
243	2193.177	16.56	25.86	6.726
244	2211.252	18.04	25.83	10.32
245	2225.892	15.05	20.88	8.4
246	2240.472	14.52	22.63	6.53
247	2256.3175	15.99	25.06	6.631
248	2273.4825	17.24	24.49	9.84
249	2290.6525	17.65	26.67	7.67

250	2306.3675	15.57	23.06	8.37
251	2324.2125	17.69	27.09	8.6
252	2344.3075	20.51	31.45	8.74
253	2363.8225	20.36	26.81	12.22
254	2376.2745	12.33	19.15	5.754
255	2385.1475	9.54	16.56	1.186
256	2396.2505	11.74	20.51	1.696
257	2412.1425	15.59	26.4	5.384
258	2431.2975	18.32	28.81	9.5
259	2450.8375	19.49	27.5	11.58
260	2467.5675	17.13	24.93	8.53
261	2483.8975	16.6	24.72	7.94
262	2501.8675	17.74	27.23	8.71
263	2520.3425	17.67	27.14	9.81
264	2539.6125	18.58	29.03	9.51
265	2559.3225	18.78	29.04	10.38
266	2577.0625	16.92	26.37	9.11
267	2591.4575	14.11	18.98	9.81
268	2606.8775	15.24	22.81	8.03
269	2621.7725	14.9	21.07	8.72
270	2635.7585	13.65	22.42	5.552
271	2651.5535	15.35	24.56	7.03
272	2668.5985	16.45	24.75	9.34
273	2685.8685	16.73	23.82	10.72
274	2699.98	14.89	21.71	6.513
275	2715.2845	15.03	24.09	6.519
276	2725.6015	13.3	19.65	0.984
277	2731.7115	5.699	13.65	-1.43
278	2738.325	5.788	13.51	-0.283